CHALMERS
UNIVERSITY OF TECHNOLOGY

Building

Propagation layer

Tunnel

XY   ZY

Estimation of correction factors of railway-induced ground-borne noise from tunnels through rock covered by soil

Master of Science Thesis in the Master's Programme Sound and Vibration

MARCUS FREDRIK ANDERSSON

Estimation of correction factors of railway-induced ground-borne noise from tunnels through rock covered by soil

Master of Science Thesis in the Master's Programme Sound and Vibration

MARCUS FREDRIK ANDERSSON

Estimation of correction factors of railway-induced ground-borne noise from tunnels through rock covered by soil
Master of Science Thesis in the Master's Programme Sound and Vibration
MARCUS FREDRIK ANDERSSON

Cover: 3d model used for simulations of train-induced ground-borne noise in Findwave.

Estimation of correction factors of railway-induced ground-borne noise from tunnels through rock covered by soil
Master of Science Thesis in the Master's Programme Sound and Vibration
MARCUS FREDRIK ANDERSSON
Department of Civil and Environmental Engineering
Division of Applied Acoustics
Vibroacoustic Research Group
Chalmers University of Technology

Abstract

Ground-borne noise is an issue in buildings in the proximity of railway tunnels. It is vibrations that are generated by railway traffic, causing sound radiation in adjacent buildings. The ability to predict ground-borne noise levels is important when planning new tunnels, since the exposure to it can have negative effects on people's health.

In this thesis, the behaviour of ground-borne noise in soils is studied, mainly through studies of engineering models and simulations in the software Findwave. In the software, a model representing a train tunnel through rock vertically below a one-floor building with basement is designed. Between the tunnel and the building is a ground layer, which thickness and material can be varied. The materials studied are: rock, loose and dense sand and clay. The layer thicknesses are 10, 20, 30, 40 and 50 m. The predicted ground-borne noise levels of the soils relative the levels of the rock can serve as correction factors for prediction models developed for wave propagation in rock.

The predicted values turned out to be low in comparison to measured values from Gårdatunneln in Gothenburg. There are some reasons why that might be, for instance the wheel and rail roughness profile used in the simulations. The calculated correction factors range within 0 to 4.2 dB, except for dense sand of 10 m, where the correction is -1.0 dB. This correction is meant to be subtracted, meaning a positive value indicates that the insertion of soil gives more damping than rock.

The validity of these results and their application to other situations are discussed. A comparison with predictions using the Ungar-Bender method shows a significant difference at short distances but more similar results further away. In general, little is known about the application of the results to other situations.

Acknowledgements

There is a number of people I would like to address, that all have contributed in one way or another in order for this piece of work to be done. First, my thanks go out to my friends and family.

I am grateful to the people at the division of Applied Acoustics at Chalmers, course mates as well as staff, who have welcomed me to the world of acoustics. It has been two very inspiring years and I especially want to thank Patrik Höstmad, who has been my supervisor for this thesis and Wolfgang Kropp.

Also, I want to show my appreciation to my colleagues at ÅF, especially Mats Hammarqvist and Martin Almgren (now at Almgren Akustikkonsult AB). Very special thanks to Erik Olsson for taking your time to hours of interesting discussions.

Another person whose contribution has been most essential is Rupert Taylor, the developer of Findwave, the software that has been used for simulations in this thesis. Thank you very much for your support.

Marcus Fredrik Andersson, Gothenburg, September 2015

Contents

Contents

1
Introduction

Railway-induced ground-borne noise is an issue in buildings near railways. In the planning of new railways, it is necessary to take into account how vibrations from these will affect nearby buildings. Also, when planning new buildings near existing railways, this is a matter of interest. For this, different prediction methods exist.

This thesis has been carried out with the consultant company ÅF. ÅF uses a calculation model that is developed for predictions of ground-borne noise for cases where building and track are separated by rock. It has been of interest to expand that model and make it applicable also for cases of different soils. This work has been about examining the possibilities to do that.

1.1 Aim/Objective

The aim is to study the behaviour of ground-borne noise in soils and to investigate the possibilities to expand prediction models that work for wave propagation in rock to work also for different types of soils.

1.2 Limitations

The choice has been made to focus on the case where the train runs through a tunnel in rock that is covered by a layer of soil. Four different soils are studied. This is done theoretically through computer simulations. The soil layers are assumed to be entirely homogenous, having the same material properties over the whole depth. This means the effect of layering is not studied, neither the interaction between layers of different soils. Unsorted sediments are not considered, nor the effect of different levels of water saturation. Frost conditions are not considered. Other types of tunnels or at-grade tracks are not studied either.

2

Background to ground-borne noise

In this chapter, the term ground-borne noise is explained. Also, health aspects and regulations concerning it are presented. This is followed up by a literature study of what factors that may influence the noise level. The last sections present some fundamentals on soils and the main components of the track and trains.

2.1   Ground-borne noise

Ground-borne noise is vibrations that are transmitted through the ground and give rise to sound radiation in structures along its propagation. Such structures may be walls, floors or other construction elements in buildings. The sound can be distinguished as a rumbling noise of low-frequency content. Other names for this phenomenon are structure-borne sound and re-radiated noise. The term re-radiated indicates that the structure is a secondary noise source and that there is a primary sound radiation going on at the source. This is the case for many sources, such as construction work and road and railway traffic that generate both airborne noise and vibrations in the ground.

Trains cause various types of airborne noise. One is rolling noise that occurs due to interaction of unevennesses of the rail and the wheel of the train as the train is in motion. In many cases this noise is loud enough to be heard through windows and low-insulating walls. In those situations it is hard to separate the ground-borne noise from the airborne noise. In buildings above railway tunnels however, where the airborne noise does not reach, the ground-borne noise can be more clearly detected. Also, ground-borne vibrations may cause objects such as plates or cutlery to vibrate and make noise, which is yet another type of noise generation that will not be dealt with further on in this report. Figure 2.1 shows how vibrations from trains spread into a building, causing perceivable noise and vibrations.
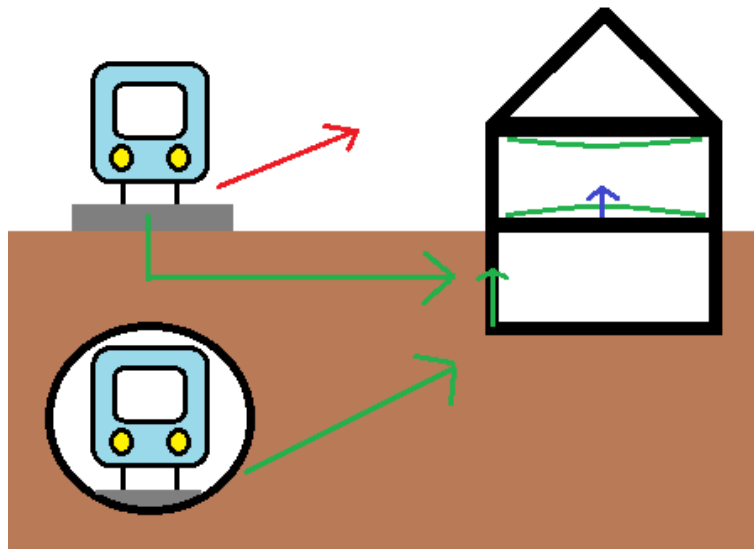
Figure 2.1: Trains causing different kinds of disturbance. Red arrow - airborne noise, green arrow - ground-borne noise and vibrations giving rise to re-radiated sound - blue arrow.

2.2 Health aspects and regulations concerning ground-borne noise

The sound pressure level of the radiated noise is usually presented A-weighted and time-weighted. Requirements are stated as either equivalent levels or maximum levels during a certain time period. Two common time constants when measuring maximum levels are SLOW (1 s) and FAST (125 ms). The notation $L_{p,AFmax}$ for instance stands for the A-weighted, maximum, sound pressure level during the period 125 ms (the letter F is short for FAST). Other notations meaning the same thing also occur.

An international ISO standard exists dealing with ground-borne noise. Its number is ISO 14837 and its title *Mechanical vibration – Ground-borne noise and vibration arising from rail system*. At the time of writing, only the first part of the standard exists, ISO 14837-1:2005. It provides general guidance in aspects such as factors that need to be considered in ground-borne noise and vibration and prediction methods [ISO 15].

In Sweden, there are no national benchmarks regarding the ground-borne noise levels, however some Swedish municipalities have their own local benchmarks. Also benchmarks can be specified for certain projects. The Public Health Agency of Sweden, Folkhälsomyndigheten, has set recommendations regarding low-frequency noise in general, specified as equivalent levels in the range of the third-octave bands 31.5 to 200 Hz, as shown in table 2.1. The stated levels are meant to be used when evaluating if there is risk of negative effects on people's health. These apply to dwellings, rooms for teaching, care or other forms of caretaking, as well as bedrooms in temporary dwellings.

Table 2.1: From FoHMFS 2014:13 [FoH 14]. Recommendations set by Folkhälsomyndigheten regarding equivalent sound pressure levels of low-frequency noise presented in 1/3-octave bands.

$f[Hz]$	31.5	40	50	63	80	100	125	160	200
$L_p[dB]$	56	49	43	42	40	38	36	34	32

In the railway tunnel project Västlänken in Gothenburg, Sweden, benchmarks have been processed and set to specify the ground-borne noise. The levels are presented as $L_{p,ASmax}$ (S indicating slow time-weighting). Depending on the difference in usage and noise sensitivity of rooms and buildings, different values have been assigned. For instance studios and music halls have stricter levels, 25-30 dBA, than offices that are used mainly during daytime, 40 dBA. The low-frequency content in the most noise sensitive buildings have to be concidered specifically for each case, as well as the total noise level. In the case of buildings where people sleep, also recommendations presented in SOSFS 1997:7 apply in addition to the total level 30 dBA. The SOSFS 1997:7 is an outdated document replaced by FoHMFS 2014:13 with a difference at 63 Hz, where the level is stated as 41.5 dB instead of 42. The specification for Västlänken in its entirety can be found in [Ham 04].

The frequency content of the ground-borne noise ranges from the lower limit of human hearing, 20 Hz, up to a few hundred Hz and sometimes even higher than that. Frequencies below 20 Hz may still be perceivable, but as feelable vibrations. According to a report on health effects of a railway segment in West Sweden [Was 03], railway-induced ground-borne noise at a maximum level of 20 dBA is usually not perceivable, at 25 dBA barely perceivable, at 30 dBA weakly perceivable and at 35 dBA clearly perceivable.

Exposure to low-frequency noise can result in "tiredness, annoyance, headache, difficulty of concentration and sleep disturbance" [SoS 08, p. 16]. A Norwegian study presented in [Aas 07] showed that both sleep disturbance and annoyance were linked to the ground-borne noise level. Norway has a requirement for the maximum level of ground-borne noise in dwellings above railway tunnels, $L_{p,AFmax}$ = 32 dB. At this level, the study showed that "20 % were slightly or more than slightly annoyed, and 4 % were moderately or more than moderately annoyed". Other factors that are believed to cause increased annoyance are the fact that the direction of the noise source cannot be determined, the relatively fast rise of the sound at a train passage [Ham 04] and how frequent the train passages are [Aas 07].

2.3   Factors influencing the ground-borne noise level

The path between vibration generation at the source and sound being radiated in a building involves a lot of factors that will influence the resulting ground-borne noise level. Hence, the prediction of ground-borne noise can be very complex.

The source of vibration is the interaction between wheel and rail and the magnitude of the vibration depends on several parameters. [Han 12] states the vehicle suspension, wheel condition, track surface, track structure and train speed to be that kind of parameters. [Mel 88] presents a prediction method for ground-borne noise from trains running in tunnels and is more specific mentioning factors such as track curvature, mass, stiffness and damping. Furthermore, it is more specific regarding the properties of the train, bringing up the stiffness and damping of the primary suspension and the mass of wheelset, bogie and car body. Also, it points out the influence of the tunnel, its dimensions, shape and thickness and also its depth. [Han 12] states that there is a difference between tracks in tunnels and tracks running on the ground surface.

The propagation path is the medium or media between the track and the receiving building, meaning it is mostly influenced by ground properties. According to [Mel 88] the ground properties that influence the ground-borne noise level are the type of soil or rock, material properties of the ground namely its density, shear modulus and loss factor and if there are any obstructions along the path. Other than that, [Han 12] mentions layering of the soil, the depth-to-water table and frost depth. Rock layer is another factor it brings up, concerning for instance the distance to the bedrock in the case of at-grade tracks and if the tunnel is founded on rock in the case of a track running in a tunnel.

The properties of the receiving building are also a matter of interest when studying ground-borne noise. [Han 12] lists the foundation type, the construction of the building and the acoustical absorption in the receiving room to be influencing factors. Other than that, [Mel 88] also brings up the natural frequencies of the floor and room size.

2.4 Some fundamentals of soils

Soils consist of grains and spaces called pores, which are filled with either gas or water or both. There may also be organic material in the composition. Soil types are divided into groups depending on their grain sizes. These groups are called soil separates and there are various classifications in the world for which particle sizes belong in which group. A geotechnical classification used in Sweden is the following:

Table 2.2: Swedish classification of soil separates [Fre 09].

Category	Clay	Silt	Sand	Gravel	Cobbles	Boulders
Grain size range [mm]	<0.002	0.002 - 0.06	0.06 - 2	2 - 60	60 - 600	600<

However, soils are usually found as mixtures of various soil separates. A descriptions such as for instance silty clay implies that the primary part of the soil composition is identified as clay, however with a significant share of silt particles. Till (morän in Swedish) is glacial sediment that is unsorted, meaning it may contain mixtures of all grain sizes, even boulders.

Permeability, the ability to allow a liquid pass through the material, is generally associated with the grain size of a soil type [Fre 09]. The finer soil types, such as clays, have low permeability, meaning they are denser, making it more difficult for a liquid to pass through. Also, it is able to hold the water longer. Soil types with larger grains, such as sand, have high permeability; meaning it is easier for a liquid to pass through. This results in the sand drying quicker than the clay [Fre 09].

The water content of a soil is of interest when studying its dynamical behaviour. Water saturation is a measure that is defined as the volume of the water in the soil over the soil's pore volume. 100 % water saturation means the soil is saturated and 0 % indicates it is entirely dry.

2.5 Track and train components

There are different principles of track construction. The most common in Sweden is the ballasted track. The rails are fastened onto sleepers which are placed in ballast of a specific depth, see figure 2.2.
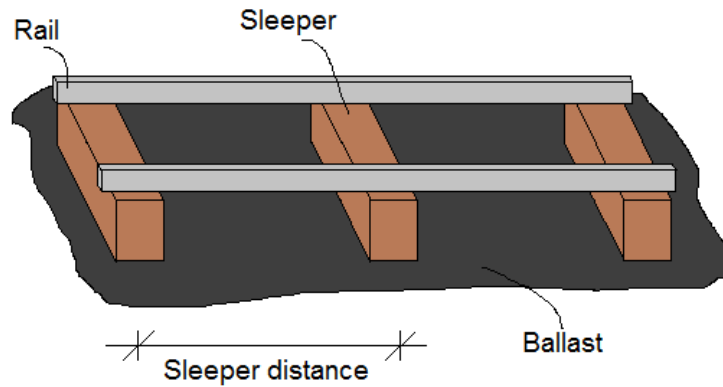

Figure 2.2: Main components of a railway track.

Trains consist of a number of suspensions and masses. These can be modelled as in figure 2.3. Unsprung mass includes the wheelset, primary mass the bogie and the secondary mass the car weight.
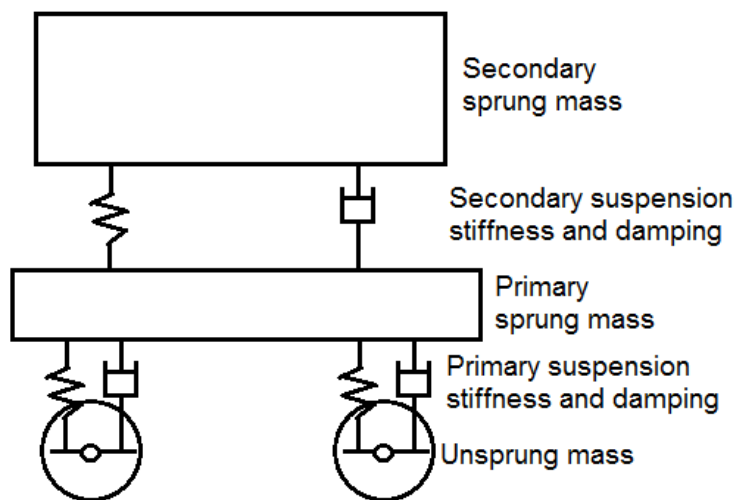

Figure 2.3: Model of a train.

3

Modelling railway-induced ground-borne noise

This chapter presents the mechanisms behind ground-borne noise, starting at the excitation at the source. One of the main parts deals with the propagation path, that is, the behaviour of vibrations in soil. Also, the last step in the path of ground-borne noise, namely its radiation in a receiving room is presented.

Another focus in this chapter is prediction methods. Special attention is given to the methods used in the next chapter.

3.1   Excitation mechanisms

The source of excitation is the interaction between track and train as the train is in motion. There are several mechanisms that contribute to the resulting excitation. The report [Lom 15] provides a thorough review of these mechanisms. It divides the total vibration into two parts, a quasi-static and a dynamic. The quasi-static contribution is from the deformation of the ground due to the weight of the train at individual axles and bogies. The report displays an examination of the contributions to the total vibration of the quasi-static and dynamic parts 16 m away from a track. In that setting, the quasi-static contribution turned out not to have significant influence above 3 Hz, which is well below the frequency range of interest in the study of ground-borne noise. It is however stated that the importance of the quasi-static contribution is higher closer to the track [Lom 15].

The dynamic contribution involves a number of mechanisms itself. [Lom 15] mentions irregularities of track and wheel surfaces and parametric excitation, which involves variations of the support stiffness along the track. The parametric excitation includes for instance the variation of stiffness due to the spacing between sleepers and at transitions between tracks. It also includes wheel flats, which are spots on the wheel that are flattened.

3.2   Wheel and rail interaction

A way to model the vertical interaction between wheel and rail is to have the wheel and rail dynamically coupled with a spring in between them, used in [Lom 15] [Tho 09]. A drawing of the model can be seen in figure 3.1. The spring is called contact spring and it represents the contact patch, which is the area where wheel and rail are in contact due to the local, elastic, deformation of the two. The excitation is due to the roughness of the rail and wheel surfaces. According to [Kur 79], poor conditions of the wheel and rail can increase the vibration levels by 10-20 dB.
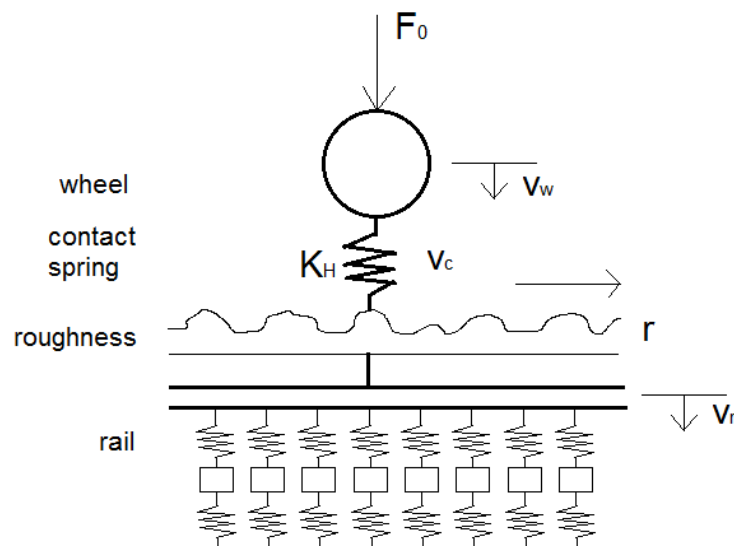

Figure 3.1: Model of the wheel and rail interaction with a contact spring. After [Tho 09].

An expression for the rail velocity found in [Tho 09] is:

$$v_r = \frac{i\omega r Y_r}{Y_r + Y_w + Y_c} \tag{3.1}$$

where $i\omega r$ is the velocity amplitude of the roughness, Y_w the mobility of the wheel, Y_r mobility of the rail and Y_c mobility of the contact spring. The contact spring mobility is expressed as follows:

$$Y_c = \frac{i\omega}{K_H} \tag{3.2}$$

where K_H is the constant called the Hertzian contact stiffness.

A resonance occurs at around 50 to 100 Hz, where the contact force has a maximum. In frequencies below it, the wheel mobility is the largest of the mobilities, whereas above it to about 1 kHz, the rail mobility is the largest [Tho 09].

3.3   Wave propagation in soils

Equation of motion

For a small element of a homogeneous, elastic and infinite medium, the equation of motion in x-direction is expressed as follows (from (3-42) in [Hal 70]):

$$\rho \frac{\partial^2 \xi}{\partial t^2} = (\lambda + G) \frac{\partial \bar{\epsilon}}{\partial x} + G \nabla^2 \xi \tag{3.3}$$

where ρ is the density of the medium, ξ the displacement in x-direction and λ and G Lamé constants. $\bar{\epsilon}$ represents:

$$\bar{\epsilon} = \frac{\partial \xi}{\partial x} + \frac{\partial \gamma}{\partial y} + \frac{\partial \zeta}{\partial z} \tag{3.4}$$

where γ and ζ are the displacements in y- and z-directions respectively. ∇^2 is the Laplacian operator in Cartesian coordinates having the following definition:

$$\nabla^2 = \frac{\partial^2}{\partial x^2} + \frac{\partial^2}{\partial y^2} + \frac{\partial^2}{\partial z^2} \tag{3.5}$$

For the equation of motion in y- or z-directions, the letter ξ in equation 3.3 is replaced by γ or ζ respectively. The Lamé constants relate to the Young's modulus, E, and Poisson's ratio, ν, in the following way:

$$G = \frac{E}{2(1 + \nu)} \tag{3.6}$$

and

$$\lambda = \frac{\nu E}{(1 + \nu)(1 - 2\nu)} \tag{3.7}$$

G also goes under the name of shear modulus.

The equation of motion has two solutions. The first represents a wave that has particle motion along its propagation direction. It has various names including: P-wave, primary wave and compression wave. Its equation is (from (3-45) in [Hal 70]):

$$\rho \frac{\partial^2 \bar{\epsilon}}{\partial t^2} = (\lambda + 2G) \nabla^2 \bar{\epsilon} \tag{3.8}$$

resulting in the expression for its velocity, c_p, being:

$$c_p = \sqrt{\frac{\lambda + 2G}{\rho}} \tag{3.9}$$

The second solution for the x-direction (similar in y- and z-direction) has the following expression (from (3-47) in [Hal 70]

$$\rho \frac{\partial^2}{\partial t^2} \left(\frac{\partial \zeta}{\partial y} - \frac{\partial \gamma}{\partial z} \right) = G \nabla^2 \left(\frac{\partial \zeta}{\partial y} - \frac{\partial \gamma}{\partial z} \right) \tag{3.10}$$

This wave is named S-wave, secondary wave and shear wave and its motion is perpendicular to its propagation direction. The shear wave velocity, c_s, is expressed as:

$$c_s = \sqrt{\frac{G}{\rho}} \qquad (3.11)$$

The shear wave can be divided into two components, one representing the motion in the vertical plane, SV-wave and the other the motion in the horizontal plane, SH-wave [Hal 12].

Wave types

The strains in soil some distance away from the track due to the train passages are relatively small, why the ground behaviour can be considered to be linear elastic when studying ground-borne noise [Lom 15]. Apart from the compression wave and the shear wave, also the Rayleigh wave belongs to the main wave types associated with ground-borne vibrations. The Rayleigh wave appears at the surface of a half-space, the ground surface, due to the interaction between the compression wave and the shear wave [Lom 15]. It propagates along the surface and its displacement decreases with the ground depth. Below a depth of about a wavelength, the Rayleigh is no longer significant [Tho 09]. Since it contains of both transversal and longitudinal motion, the resulting motion is circular. The speed of the Rayleigh way can be approximated as (2.6 in [Lom 15]):

$$c_r \approx \frac{0.862 + 1.14\nu}{1 + \nu} c_s \qquad (3.12)$$

where ν is the Poisson's ratio and c_s the shear wave speed. The compression wave is the fastest. The shear wave and Rayleigh wave are closer in wave speed, although the Rayleigh wave is somewhat slower.

Damping

Two types of damping behaviour are associated with wave propagation in soils, geometrical and material damping. Geometrical damping means a decrease in amplitude of the wave front due to geometrical spreading over an increasing volume. In other words, there are no losses in the total wave energy. Material damping however implies energy losses in the wave energy. Friction between soil particles causes energy dissipation in the propagating wave. The dissipated wave energy is transformed into heat. A hysteresis loop, as can be seen in figure 3.2, shows the relation between shear stress and the shear strain during a cycle load. The area within the loop is a measure of the energy loss [Hal 12]. The material damping is expressed in the loss factor, η, as follows:

$$\eta = \frac{E_{dis}}{2\pi E_{max}} \qquad (3.13)$$

where E_{dis} is the dissipated energy in a cycle and E_{max} the total strain energy.
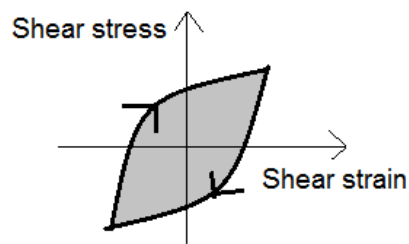
Figure 3.2: A hysteresis loop.

Refraction and reflection

At the border between two ground layers with different material properties, a part of an incoming wave will be transmitted into the other layer, which is called refraction. The other part will be reflected and remain in the current layer. The amplitudes and direction of the refracted wave depend on the angle of incidence of the wave, stiffness and density of the two layers [Hal 12]. Equation 3.19 in the following section about the Ungar-Bender method is a way to represent the damping due to reflections at the border of two ground layers.

Resonances in soil

A soil layer on top of bedrock has eigenfrequencies that can be approximated by (from 2.1.9 in [Hal 12]):

$$f_{eig,n} = \frac{(2n+1)}{4H} c_s \tag{3.14}$$

where n is a number 0, 1, 2... and H is the thickness of the soil layer. The equation holds for an SH-wave propagating in the vertical direction [Hal 12]. Excitation at these resonance frequencies can cause amplified displacements and motion even at low levels of excitation.

3.4 Sound Radiation

The radiated power due to vibrations from a surface is given by:

$$W_{rad} = \frac{1}{2}\sigma S \rho_{air} c_{air} \langle v \rangle^2 \qquad (3.15)$$

where σ is the radiation efficiency, S is the area of the surface, ρ_{air} the density of air, c_{air} the wave speed in air and $\langle v \rangle^2$ the spatially averaged mean-square velocity of the vibration.

The radiation efficiency is a frequency-dependent quantity that describes the vibrating structure's ability to excite the contiguous air. Sound radiation from plate-like structures, such as walls and floors, is however a complex matter that depends on a number of factors. Bending waves is the wave type that is mainly responsible for the radiation of sound and the only wave type that is needed to study when studying frequencies that are not very high [Mul 13]. The bending wave is also called flexural wave and causes deformation perpendicular to the propagation direction. For a mathematical description of bending waves, [Cre 05] is recommended. At the so-called coincidence frequency, the wavelength of the bending wave in the plate is equal to the wavelength of the contiguous air. In infinite plates, below the coincidence frequency, the bending waves only cause near-field excitation of the air. In finite plates however, there will be sound radiation from borders such as corners and edges and also low-frequency modes even below the coincidence frequency. Above it, the plate is able to excite the air and the wavelength in the plate is shorter than the wavelength in air. Other factors that influence the radiation from plates are the type of excitation, how they are supported and the presence of discontinuities [Mul 13].

3.5 Prediction methods

Railway-induced ground-borne noise is a problem in inhabited areas. Hence, there is an interest in being able to predict ground-borne noise levels when designing new railways. A number of different prediction methods exist and are practiced in railway projects. The choice of method depends on the situation, for instance the desired degree of accuracy and time available.

One way of predicting the ground-borne noise at a site is to perform measurements at a site with similar properties. The accuracy of this type of prediction depends largely on how close the properties of the measured site and the site of prediction are. Since there is a large number of factors that influence the ground-borne noise, one has to be aware of that even small deviations can have notable impact on the results.

Empirical methods are common for calculating ground-borne noise and vibrations. In general they are easy and fast to use, but the accuracy may not be very high. However, for conservative estimates it is a useful tool. In empirical models, the path between source and receiver is described as a series of transfer functions. The factors that have an impact on the resulting level are represented as correction factors. Some models found in scientific papers are presented in [Ung 75], [Kur 79] and [Mel 88].

Another method is to make a numerical model of the site and simulate the train passage. Theories used are for instance Finite Element Method (FEM), Finite Difference Method (FDM) and Boundary Element Method (BEM). With a well functioning theory, the accuracy of the results depends on the quality of the input data. The software package Findwave was used for predictions in a report by the company Crossrail [Cro 04], in which predicted results were compared to measured. In the report, a point was chosen for predictions and measurements of the velocity level, which was seen as the velocity level in the floor of a hypothetical building. By subtraction of 27 dB, a so called "pseudo-groundborne noise level" was calculated. The two presented results showed a difference of 3 dBA in one case, but in the other the difference between measured and predicted results was just 0.3 dBA [Cro 04].

3.6 Findwave

Findwave is a software package that is used to predict noise and vibrations from railways and is developed by Rupert Taylor Ltd. It is based on the, FDTD, Finite Difference in Time Domain method. Modelling is done in a space built up by small three-dimensional cells of the same dimensions. This allows modelling of three-dimensional scenarios. The cells are assigned a material with properties such as compression wave speed, shear wave speed, loss factor and density. From these parameters, the Lamé constants and cell masses are automatically calculated.

The vehicle used for simulations is provided in a separate file. It is assigned parameters such as values for characteristic masses, stiffnesses, damping, axle placement, vehicle speed and inclination. The inclination determines the distribution of the load on the two rails.

Equation of motion on finite difference form

The mathematical theory behind Findwave is presented in [Tay 04]. An essential part is how the differential operator is approximated as:

$$\frac{\partial \xi}{\partial x} \approx \frac{x\left(i, j, k\right) - x\left(i - 1, j, k\right)}{\Delta x} \tag{3.16}$$

where ξ is the displacement along the x-axis, $x\left(i, j, k\right)$ and $x\left(i - 1, j, k\right)$ refer to positions on the x-axis, i, j and k are indices and Δx the distance between the two positions. By inserting this approximation in the equation of motion (equation 3.3) it is said that the equation is written on finite difference form [Tay 04].

3.7 Ungar-Bender method

The Ungar-Bender method is presented in the paper [Ung 75]. It presents a method for calculating the attenuation in the ground from a railway tunnel. Using this method, it is possible to estimate a frequency response function of the vibration velocity level, L_v, in the basement floor of a building, as long as the spectrum at the tunnel wall is known. The method assumes that the wave type that contributes the most to the vibration is the compression wave. The attenuation due to geometrical damping is (from (1) in [Ung 75]):

$$A_g = 10log\left(\frac{r_0 + x}{r_0}\right) \tag{3.17}$$

where r_0 is the distance from the middle of the tunnel to the outside of the tunnel wall and x is the distance from the outside of the tunnel wall to the observation point. The material damping is given in this equation (from (2) in [Ung 75]):

$$A_m = 10log\left(e^{\frac{-2\pi f x \eta}{c_p}}\right) \tag{3.18}$$

where f is the frequency, η the loss factor of the ground and c_p the compression wave speed. In the case of several layers, the following equation gives the attenuation due to the change of impedance, A_i, between those layers (from (3) in [Ung 75]):

$$A_i = 20log\left[\frac{1}{2}\left(1 + \frac{\rho_2 c_{p,2}}{\rho_1 c_{p,1}}\right)\right] \tag{3.19}$$

where ρ_i is the density of layer i $c_{p,i}$ the compression wave speed in layer i. This equation holds only if the propagation length is much larger than the so-called decay distance, L_{dec} having the following equation (from (4) in [Ung 75]):

$$L_{dec} = \frac{c_p}{2\pi f \eta} \tag{3.20}$$

The total attenuation is the sum of the contributions from equations 3.17, 3.18 and 3.19.

4

Simulating railway-induced ground-borne noise from a train propagating through a tunnel in rock

This chapter presents a model in Findwave that has been developed to study ground-borne noise in soils. The model is also used for finding correction factors that compensate for the difference in ground-borne noise level due to propagation in soils in prediction models that are developed for propagation in rock.

4.1   Overview of the model

To study the behaviour of ground-borne noise propagating in soils, Findwave is used. The same model is used for the entire study, however with some modifications. It features a train tunnel, a propagation layer and right above the tunnel a building, in which the ground-borne noise level and vibration velocity level are studied. A graphical overview of the model can be seen in figure 4.1. Since the focus in this study is the propagation in soils, the main principle of the model is to only allow modifications of the propagation path. Parameters such as track construction, vehicle type, vehicle speed, building construction and loss factor in the receiving room are kept constant during all simulations.
Modelling in Findwave is done in a 3d mesh built up by small cells, which dimensions and total number are assigned initially. In this model, the cell dimensions in x-, y- and z-direction are 0.25, 0.25 and 0.2 m. The number of cells in the same directions is 60, 250 and 75, resulting in total dimensions of the model being 15, 62.5 and 15 m.
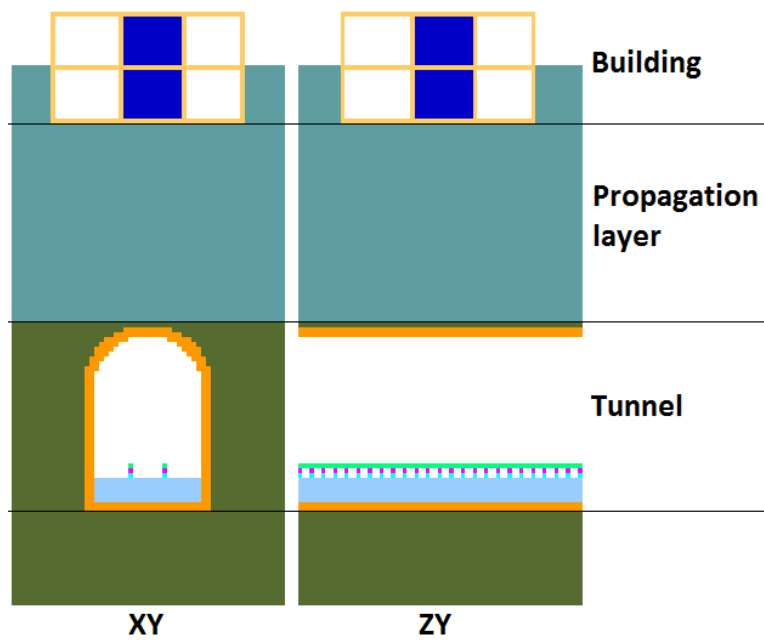
Figure 4.1: Overview of the Findwave model showing the xy- and the zy-planes.

The building

The building has two floors, one below ground and one above. It is 10 m long and 10 m wide. Its height above ground is 2.75 m. The material used in walls, floors and roof is concrete. All building elements have the thickness of one cell, meaning that the walls in the xy-plane are a bit thinner (0.2 m) than the other building elements (0.25 m). This corresponds to the cell dimensions as described previously. Material data associated with the building are found in table 4.1.

The room of interest is the middle room on ground floor, where the results of the ground-borne noise level are obtained. The interior dimensions of the room are 3 m by 3 m and height 2.5 m. The loss factor of the air in the room is assigned a value that is calculated from equation 4.1 (from [Tay 04]):

$$\eta \approx \frac{4.4}{RT * f} \qquad (4.1)$$

where RT is the reverberation time and f the frequency. A reverberation time of 0.5 s at 100 Hz are the parameters used in the equation. The ground-borne noise level is evaluated in a total of 30 points in the middle of the room and averaged.

Table 4.1: Material data used in the building. Values used are predefined in Findwave unless otherwise stated. Comments: [a] Described in the text above.

Material	Colour code	$c_p[m/s]$	$c_s[m/s]$	$\rho[kg/m^3]$	$\eta[-]$
Concrete	Yellow	3600	2200	2400	0.05
Air, receiving room	Dark blue	344	1	1.18	0.09 [a]
Air, other	White	344	1	1.18	0.09

The frequency of the room modes can be calculated from the following equation:

$$f_0 = \frac{c_{air}}{2} \sqrt{ \left(\frac{n_x}{L_x} \right)^2 + \left(\frac{n_y}{L_y} \right)^2 + \left(\frac{n_z}{L_z} \right)^2 } \qquad (4.2)$$

where c_{air} is the speed of sound in air, n_x, n_y and n_z are mode orders and L_x, L_y and L_z room size in x-, y- and z-direction. With the properties of the receiving room, the first modes are the following:

Table 4.2: The first 12 room modes with $c_{air} = 344$ m/s, $L_x = L_z = 3$ m and $L_y = 2.5$ m and which 1/3 octave band they belong to.

Mode order (n_x, n_y, n_z)	Frequency [Hz]	1/3 octave band [Hz]
(1, 0, 0)	57.3	63
(0, 0, 1)	57.3	63
(0, 1, 0)	68.8	63
(1, 0, 1)	81.1	80
(1, 1, 0)	89.6	100
(0, 1, 1)	89.6	100
(1, 1, 1)	106.3	100
(2, 0, 0)	114.7	125
(0, 0, 2)	114.7	125
(2, 0, 1)	128.2	125
(1, 0, 2)	128.2	125
(0, 2, 0)	137.6	125

Boundary conditions

The boundary conditions in both ends of both the x-, and y-axes are set to be absorptive, meaning that the wave fronts going out of the model are absorbed. The boundary condition in both ends of the z-direction is called end-to-end. This means that the ends are connected so that what goes out of the model in one end comes in from the other end and vice versa.

Tunnel

Tunnel dimensions have been chosen in order to freely fit a train. The height above track is 6.5 m and its width is 5.5 m. The thickness of the tunnel roof is 0.75 m.

Vehicle

The vehicle used for simulations is a model of a freight train car, which data can be found in table 4.3. The speed of the vehicle is 80 km/h. The end-to-end connection boundary condition results in an infinite number of cars being connected into an infinitely long train set. However, during the simulation time not even two entire cars have time to pass through the model.

Table 4.3: Vehicle data representing a freight train car. Parameters obtained from the company.

Total length	15 m
1st axle	0 m
2nd axle	9 m
3rd axle	15 m
Vehicle mass per wheel	7750 kg
Vehicle secondary suspension stiffness	$4.0 * 10^6$ N/m
Secondary suspension damping	20000 Ns/m
Sprung mass of bogie per wheel	2000 kg
Stiffness of primary suspension	$2.0 * 10^6$ N/m
Primary suspension damping	10000 Ns/m
Unsprung mass per wheel	1000 kg
Hertzian contact stiffness	$1.2 * 10^9$ N/m
Stiffness of primary damper bushes	$9.5 * 10^6$ N/m

Track construction

The track construction features rails, rail pads, sleepers and a ballast layer. The material data can be found in table 4.4. The ballast layer has a total thickness of 1.25 m. The sleeper distance is 0.6 m. Since the cell size in z-direction, the direction of train propagation, is 0.2 m, the sleeper distance in terms of cells results in having sleepers in every three positions along the z-axis. Between rail and sleeper is a rail pad. The distance between the rails is 1.5 m. The track is straight and not inclined, meaning the axle load is evenly distributed on the two wheels.

Table 4.4: Material data used in the track. Values used are predefined in Findwave unless otherwise stated. Comments: [a] Values obtained from the company and scaled to the cell dimension in this study.

Material	Colour code	$c_p[m/s]$	$c_s[m/s]$	$\rho[kg/m^3]$	$\eta[-]$
Rail	Light green	7530	4095	2440	0.01
Rail pad [a]	Magenta	2740	1120	40	0.05
Sleeper	Light blue	3600	2200	2400	0.06
Air	White	344	1	1.18	0.09
Ballast	Light grey/blue	408	263	1800	0.03

Other parameters

Some other parameters that are used in the model, involving damping and evaluation time are listed in table 4.5. The Boltzmann constants and relaxation times are constants that are involved in the damping algorithm that is used to achieve frequency dependent damping. The damping principle is described in [Tay 04].

Table 4.5: Other parameters used in the model. All values predefined in Findwave.

Boltzmann constant	3.872
Boltzmann constant	0.709867
Boltzmann constant	0.790533
Relaxation time	0.00016 s
Relaxation time	0.0016 s
Relaxation time	0.014 s
Stiffness frequency	4 Hz
Time step	$7.63 * 10^{-6}$ s
Number of time steps	131072
Total evaluation time	1 s

4.2 Material study

The materials studied here are rock, loose sand, dense sand, loose clay and dense clay. For each material, the spectrum in the receiving room from the radiated ground-borne noise is calculated. This is done for the distances 10, 20, 30, 40 and 50 m between the outer wall of the tunnel and the basement floor. Also the total levels are calculated. The material parameters used are for water saturated soils and are found in table 4.6:

Table 4.6: Material data used for the propagation layer. Wave speeds and densities found in [Hal 12] (table 2.2.6). The loss factors of the soils are based on loss factors predefined in Findwave for other types of sand and clay. The loss factor of rock found in [Ung 75].

Material	$c_p[m/s]$	$c_s[m/s]$	$\rho[kg/m^3]$	$\eta[-]$
Rock	5250	2750	2400	0.01
Sand, loose	1500	175	1500	0.05
Sand, dense	1850	525	2050	0.05
Clay, loose	1500	130	1800	0.05
Clay, dense	1750	400	2050	0.05

4.3 Correction factors for attenuation in soil

The study in the previous section evaluates the ground-borne noise level in a building on a variable ground layer that is called propagation layer. The only difference between the simulations is the material used in the variable ground layer. All other parameters are kept the same. This is studied for five thicknesses of the propagation layer.

A prediction model that is valid for situations where rock is the material of wave propagation, could be expanded to work also for soils. With the assumption that the properties of the rock used in the previous section are the same as in that prediction model, the difference between the values for the soils relative to rock, could serve as correction factors in that prediction model. In that case, a correction factor for the total level for each of the soils studied could be calculated from this equation:

$$L_{corr,soil} = L_{p,A,rock} - L_{p,A,soil} \qquad (4.3)$$

where $L_{p,A,rock}$ and $L_{p,A,soil}$ are the total levels of the ground-borne noise from propagation in rock and a type of soil respectively and $L_{corr,soil}$ the correction factor for that type of soil. It should be noted that the obtained correction factor is calculated for the specific case modelled in this study and other settings might have other corrections.

4.4 Influence of the loss factor

The influence of the loss factor is studied for the case of loose sand at the distance of 40 m. The loss factors used are: 0.03, 0.04, 0.05, 0.06 and 0.07. Simulations are performed using each of these loss factors for the propagation layer, keeping all other parameters constant. The results from this study are from early preliminary simulations in which the loss factor of the air in the receiving room had a different value, 0.009. It was later changed to 0.09 to simulate more a more realistic case for residential units. Hence, the results look a bit different from those in the previous section.

4.5 Ungar-Bender comparison

The validity of the results in the material study is best examined by comparing results from in situ measurements of cases with the same setting as the model. However, this method has not been available for this thesis. Instead, the choice has been made to compare the obtained attenuation in the ground using Findwave to what the Ungar-Bender method predicts using the same material and geometrical data. This is not a proper validation since both methods are theoretical and none of them can be said to be an entirely correct method. However, the comparison can serve as an indication on whether the obtained results are reasonable or not. The comparison is done by subtracting the predicted damping of the Ungar-Bender method from the spectrum of the vibration velocity levels in the outer wall of the tunnel. This way, a new spectrum is obtained which is the predicted spectrum of the vibration velocity levels in the floor of the basement. Findwave is also instructed to calculate the vibration velocity levels in the basement floor so that the predicted values of the two methods can be compared.

4.6 Other

It is of interest to see how the vibration velocity varies throughout the model. For the case of rock and loose sand, at 10 and 40 m, the vibration velocity in y-direction is obtained for the rail, tunnel floor below the ballast layer, outer wall of the tunnel, basement floor, ground level floor and roof of the building. These locations are displayed in figure 4.2. It is also of interest to compare the vibration velocities of the surfaces in the room to the resulting sound pressure level. This is studied for loose sand and rock at 10 m.
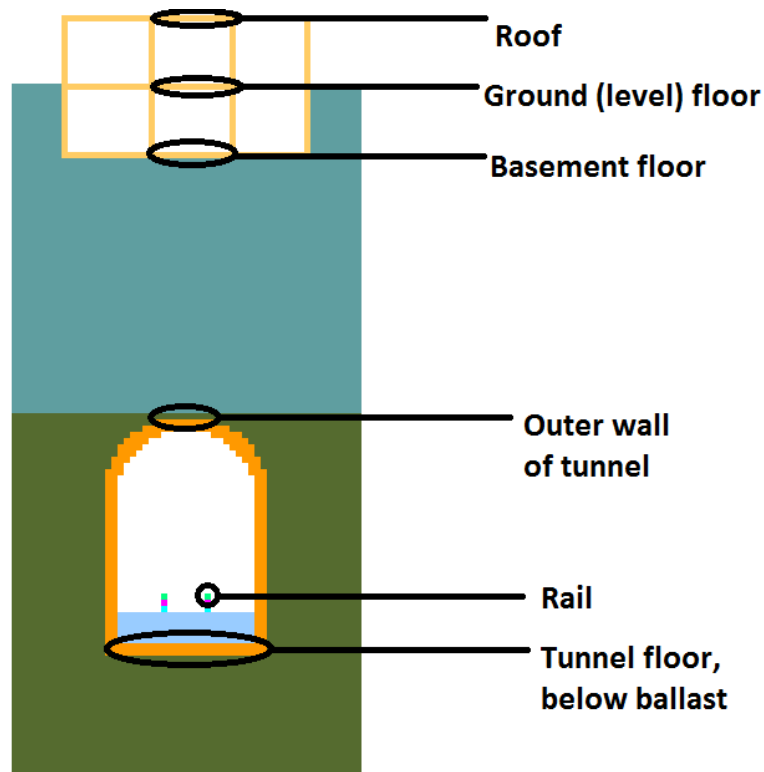
Figure 4.2: Locations where vibration velocity levels in y-direction (vertical) are studied.

5

Results

This chapter presents the results from the studies.

5.1 Material study

Studying the A-weighted ground-borne noise level, it turns out that the levels are lower than what one would expect. The loose sand and clay have very similar spectra. Except for that, the shape of the curves in the spectra is unique for each material. The shape tends not to change that much with increasing distance, but the level is lowered. This is shown in figures 5.1, 5.2 and 5.3.
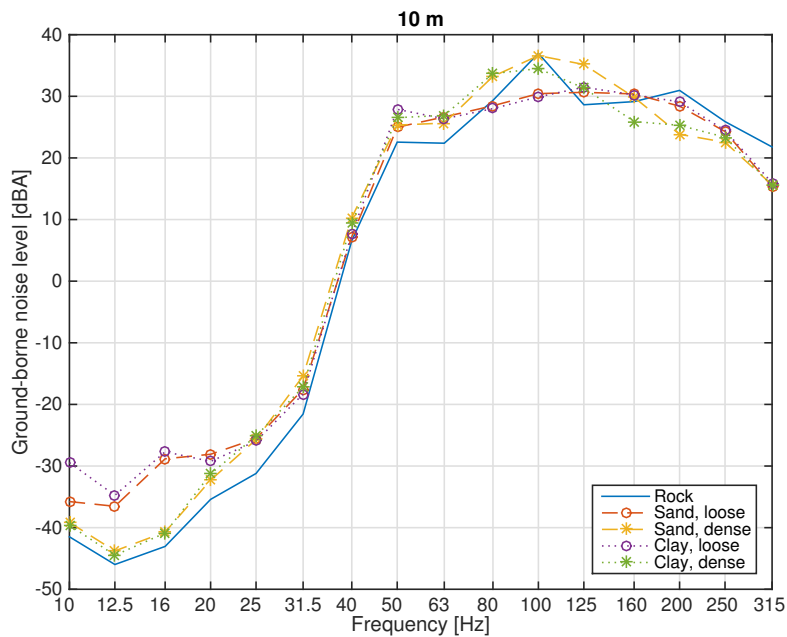
Figure 5.1: A-weighted ground-borne noise levels [dB re. 20 μPa] for all studied materials at a distance of 10 m.
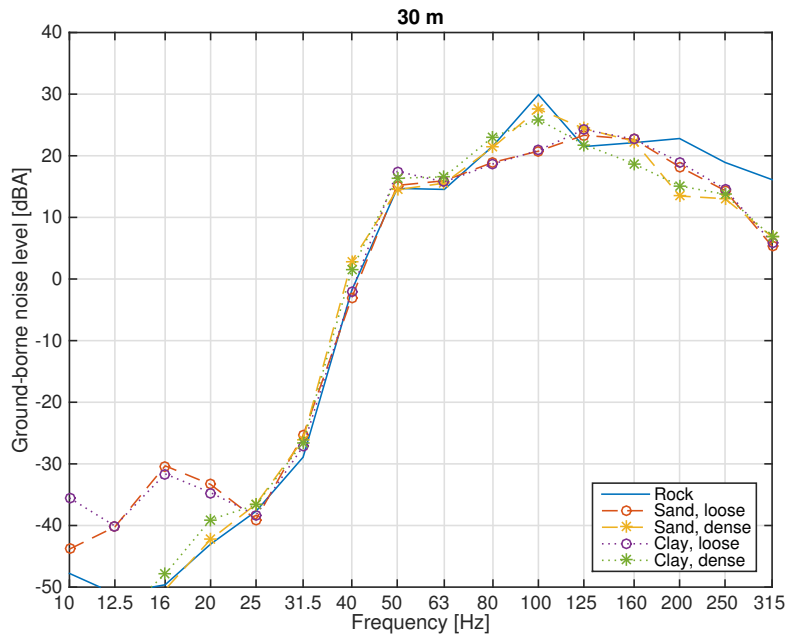
Figure 5.2: A-weighted ground-borne noise levels [dB re. 20 μPa] for all studied materials at a distance of 30 m.
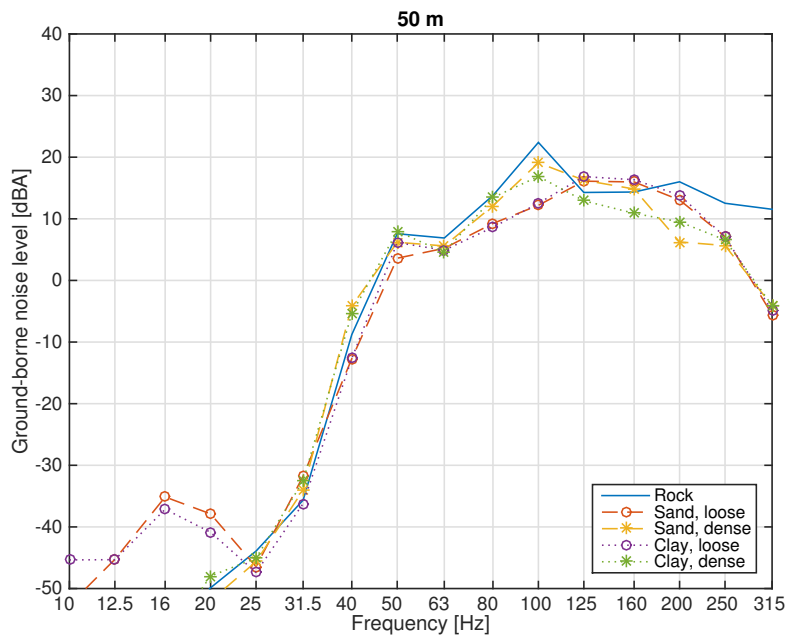
Figure 5.3: A-weighted ground-borne noise levels [dB re. 20 μPa] for all studied materials at a distance of 50 m.

Looking at total levels, rock is the material that causes the highest levels at all distances except for at 10 m, where the dense sand has the highest levels. All materials have a steady decrease with distance, in most cases 4 to 5 dB per 10 m increase of the distance. The difference between loose sand and clay is small as implied in the spectra. The ground-borne noise level in the dense sand is higher than for the loose sand over the studied distances. The dense clay however, turns out to cause higher noise levels than the loose clay only the first 30 m. At 40 m both clays have the same level and at 50 m the ground-borne noise is actually more damped in the dense clay than in the loose.
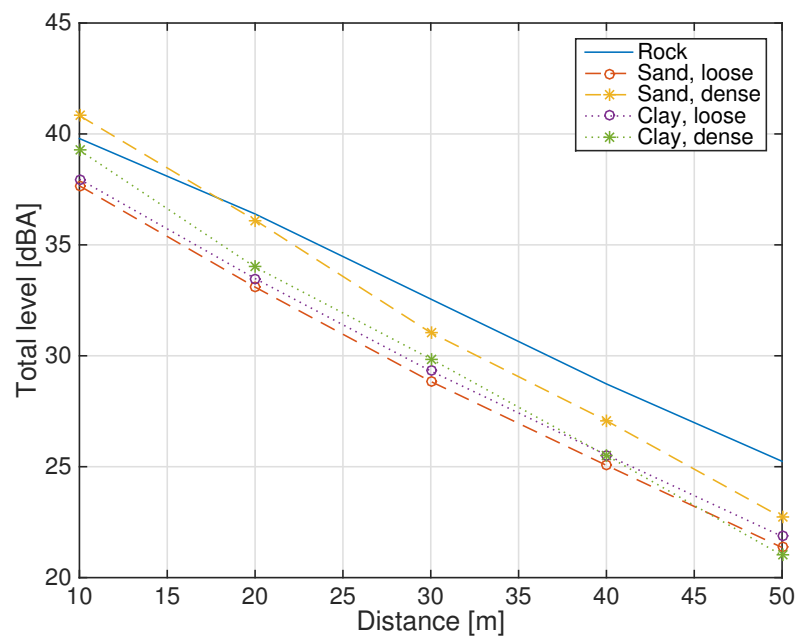
Figure 5.4: Total A-weighted ground-borne noise levels [dB re. 20 μPa] for all studied materials. Variation over distance.

Table 5.1: Total A-weighted ground-borne noise levels [dB re. 20 μPa] for all studied materials. Variation over distance.

Material	$L_{p,A}$ [dBA] at distance				
	10 m	20 m	30 m	40 m	50 m
Rock	39.8	36.4	32.6	28.7	25.2
Sand, loose	37.7	33.1	28.8	25.1	21.4
Sand, dense	40.8	36.1	31.0	27.1	22.7
Clay, loose	38.0	33.5	29.3	25.5	21.9
Clay, dense	39.3	34.0	29.9	25.5	21.0

5.2 Correction factors for attenuation in soil

The correction factor is calculated as the difference in ground-borne noise level between rock and the soils as presented in the previous chapter. The correction factor is supposed to be subtracted in the prediction model. Positive values indicate that there is more damping in the soil than in the rock material. At 10 m the dense sand causes a 1 dB increment. At all other distances and for all materials, the insertion of the soil reduces the total level.
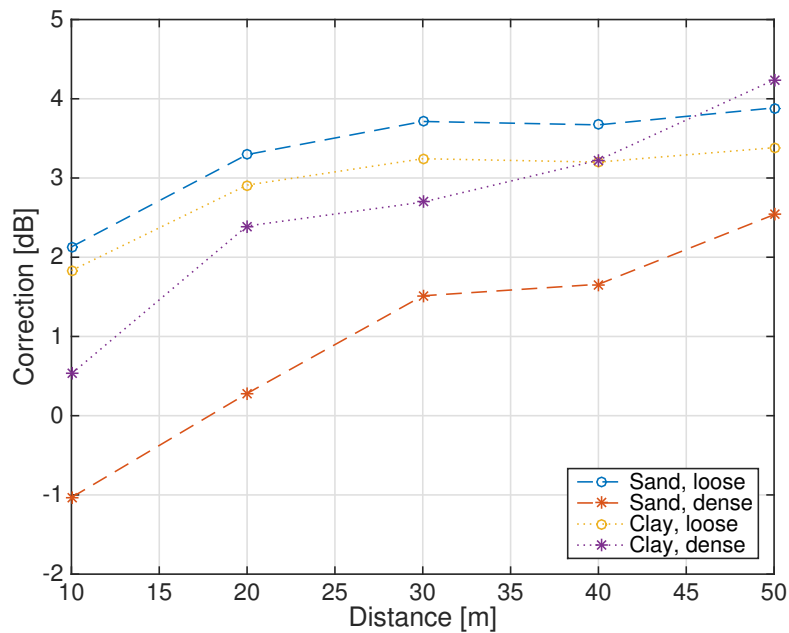
Figure 5.5: Correction factors from the total ground-borne noise levels of the soils relative to rock.

Table 5.2: Correction factors from the total ground-borne noise levels of the soils relative to rock.

Material	$L_{corr,soil}$ [dB] at distance				
	10 m	20 m	30 m	40 m	50 m
Sand, loose	2.1	3.3	3.7	3.7	3.9
Sand, dense	-1.0	0.3	1.5	1.7	2.5
Clay, loose	1.8	2.9	3.2	3.2	3.4
Clay, dense	0.5	2.4	2.7	3.2	4.2

5.3 Loss factor

The influence of the loss factor is shown in the spectra in figure 5.6. Material damping increases with frequency and the lower the value of the loss factor, the higher the ground-borne noise level. These simulations were done for the case of loose sand and at the distance of 40 m. Since the material properties of the air in the receiving room are different, these results cannot be properly compared to the ones obtained in the material study. However it can be seen that the choice of loss factor has a significant influence on the results. The total levels can be seen in table 5.3.
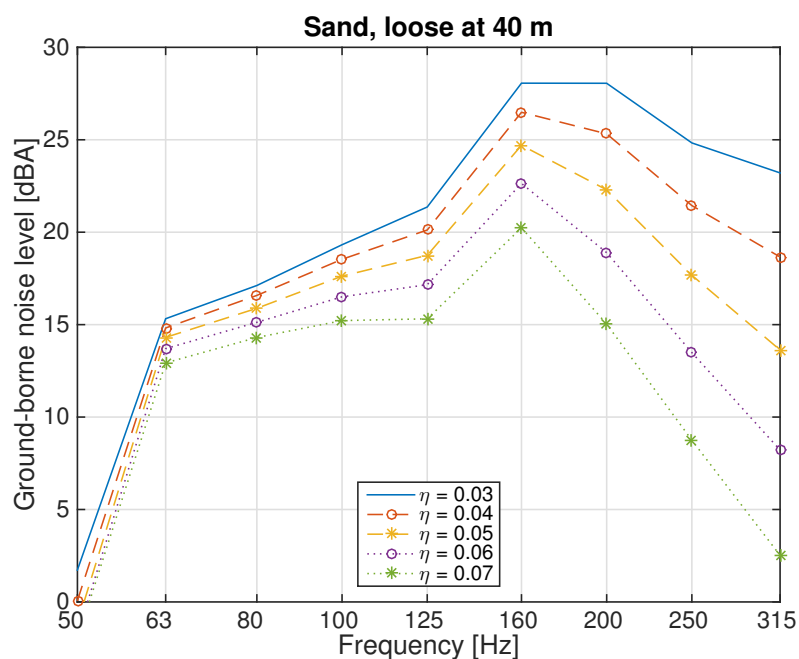
Figure 5.6: Difference in ground-borne noise level [dB re. 20 μPa] due to varying the value of the loss factor for the case of loose sand at a thickness of 40 m.

Table 5.3: Difference in ground-borne noise level [dB re. 20 μPa] due to varying the value of the loss factor for the case of loose sand at a thickness of 40 m.

$\eta[-]$	$L_{p,A}[dBA]$
0.03	33.2
0.04	31.0
0.05	28.7
0.06	26.5
0.07	24.2

5.4 Ungar-Bender comparison

A general comment regarding the comparison between Ungar-Bender and the Findwave prediction is that the Ungar-Bender method gives more reduction at the shorter distance. This is clearly shown for the case of rock in figure 5.7 and for loose sand in figure 5.10. At 40 m, the predictions are more similar, yet not identical. Figure 5.8 shows the case for rock and 5.9 for loose sand. In most frequency bands, the difference is within 5 dB for these two cases. The comparisons for the other materials can be found in the appendix, section A.2.

The actual damping is shown in figure 5.10. It displays the exponential behaviour of the Ungar-Bender prediction. In low frequencies, there is little or no material damping, why the damping in the low frequencies mostly depends on the geometrical damping. The influence of the material damping increases with frequency and distance, which explains the sharper curve at 40 m compared to at 10 m. The damping according to Findwave is by no means as smooth as the Ungar-Bender method predicts. Both Findwave curves have peaks and troughs, although the 10 m curve is a bit more even. A major difference at 10 m is the fact that Findwave calculates higher levels in the basement than in the tunnel wall (negative values in the figure), whereas Ungar-Bender predicts at least 5 dB reduction. At 40 m the curves intersect and are closer, but there are still considerable differences.
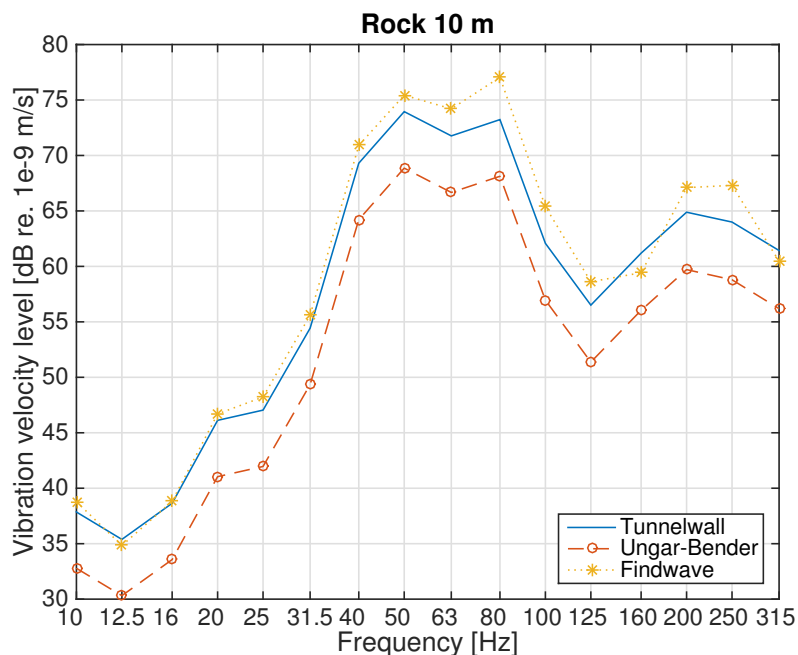

Figure 5.7: Comparison of simulated values and calculated values using the Ungar-Bender method for rock 10 m. NB! Vibration velocity levels.
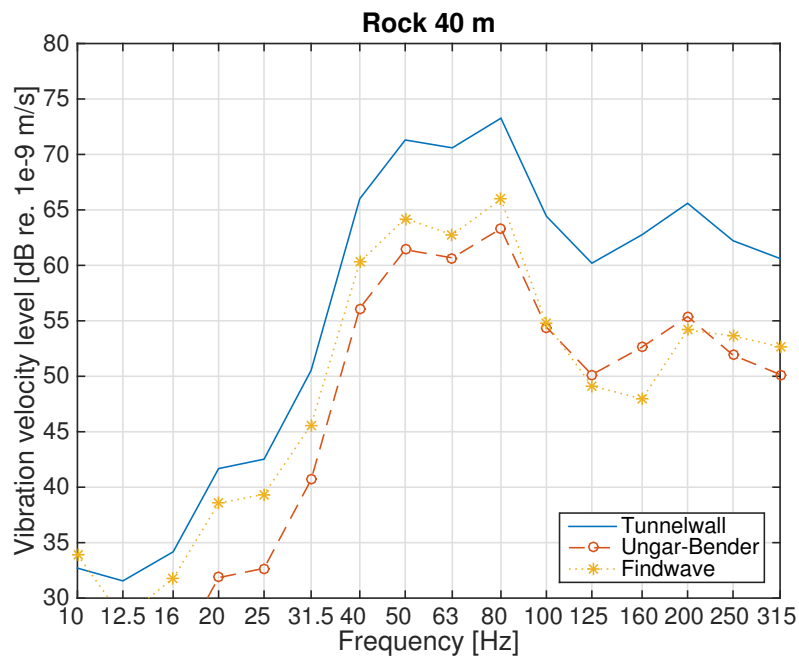
Figure 5.8: Comparison of simulated values and calculated values using the Ungar-Bender method for rock 40 m. NB! Vibration velocity levels.
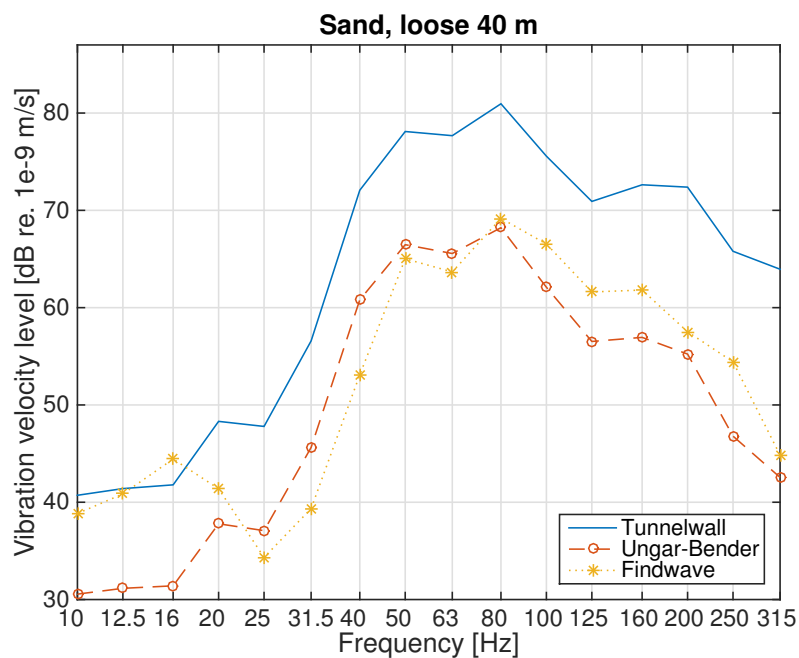

Figure 5.9: Comparison of simulated values and calculated values using the Ungar-Bender method for loose sand 40 m. NB! Vibration velocity levels.
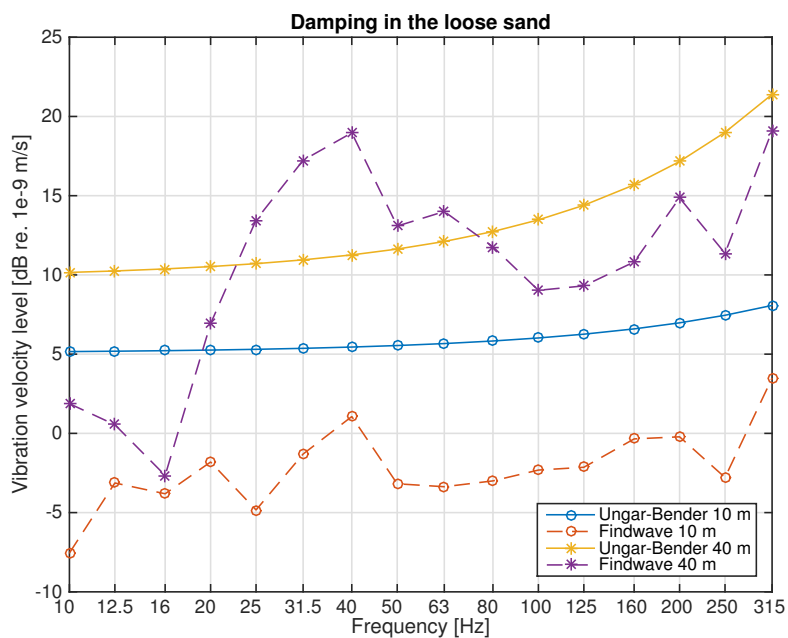
Figure 5.10: Comparison of damping from simulated values and calculated values using the Ungar-Bender method for loose sand at 10 and 40 m. NB! Vibration velocity levels.

5.5 Other results

Figure 5.11 shows how the vibration velocity levels vary between different parts of the model for the case of 40 m loose sand. In the rail, the level is close to 140 dB from 40 Hz and up to the upper limit. Below 40 Hz the level is lower, yet above 100 dB. Note that these curves are not weighted in any way. In the tunnel floor, below the track construction, the level is attenuated by around 40 to 60 dB. In the outer wall of the tunnel, the levels are lower and in the basement floor even lower than that.
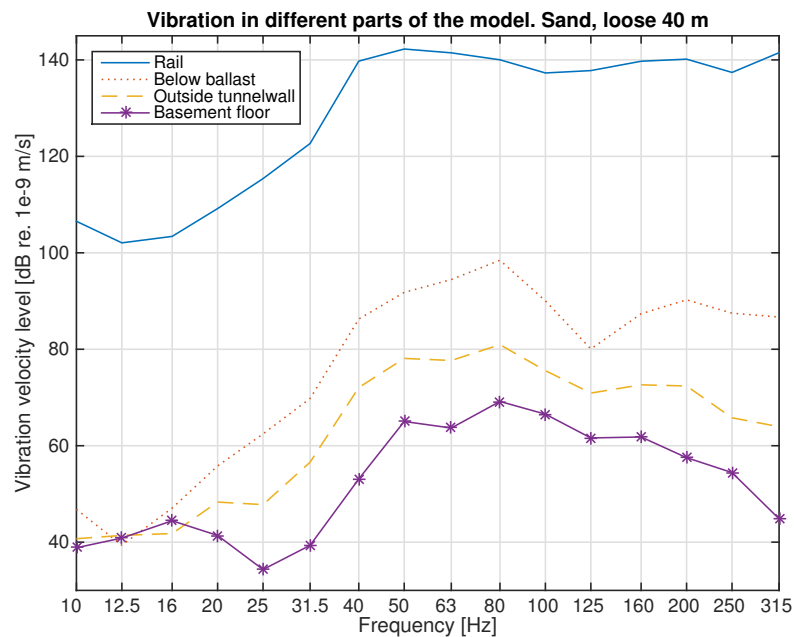
Figure 5.11: Variation of the vibration velocity levels at different parts of the model in the case of 40 m loose sand.

Comparing the vibrations in y-direction of the different floors and roof in the building reveals distinct differences due to the type of ground. Beginning with rock, figure 5.12, starting at 40 Hz there are quite big differences between the two floors and the roof. The lowest levels are found in the basement floor and the highest in the roof. A large peak is found at 100 Hz, which represents the highest level at each distance. The shapes of the curves are very similar at the two distances, although the levels are different.
Looking at the loose sand, figure 5.13, it is noticeable how the curves are more similar within the same distance compared to the case of rock. The highest levels are still found in the roof, but there is no peak at 100 Hz as in the case of rock. Instead, the highest values are found at 63 and 80 Hz. Shape wise there are only some small differences between the distances.
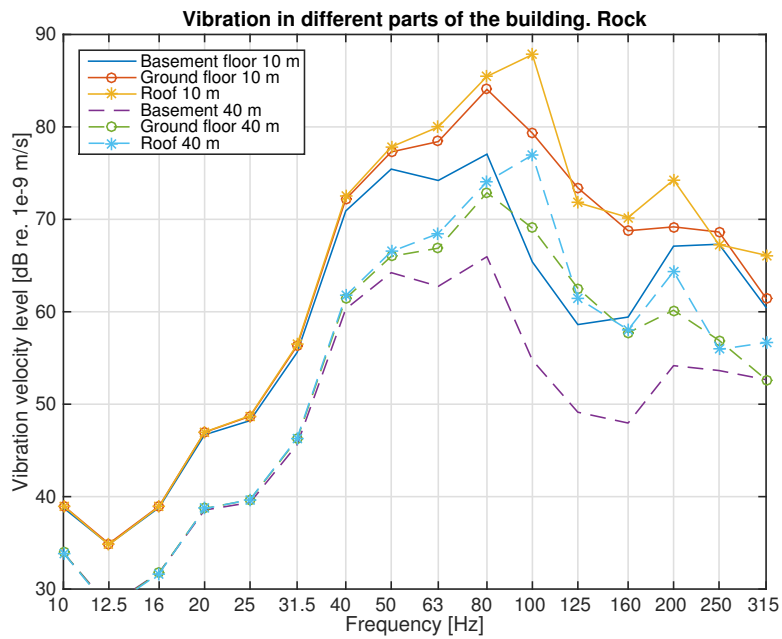
Figure 5.12: Variation of the vibration velocity levels in the horizontal building elements for rock 10 and 40 m.
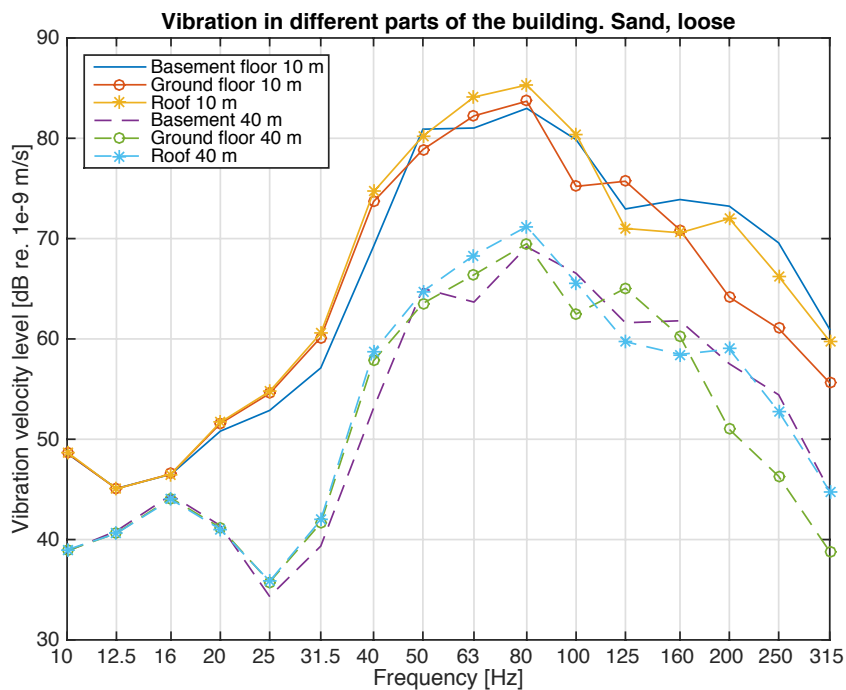

Figure 5.13: Variation of the vibration velocity levels in the horizontal building elements for loose sand 10 and 40 m.

Figures 5.14 and 5.15 show the vibration velocity levels in the walls, floor and roof of the receiving room, along with the sound pressure level (not A-weighted) in the room. The walls in the zy-plane of the model have a thickness of 0.25 m and the walls in the xy-plane 0.2 m. In both cases, the thinner wall displays higher levels than the other surfaces below 25 Hz. Above, both wall types behave more similarly, although there are some smaller differences. Especially in the case of loose sand, the levels are higher in the horizontal surfaces than the walls in the frequency region of interest to ground-borne noise. In the case of rock, the vibration velocities in the walls, especially the thinner, are closer to the ones of the roof and floor. The sound pressure levels have a peak at 50 Hz for both materials. This peak is not visible in any of the vibration velocities. However, the peak of the roof at 100 Hz in the case of rock can also be seen in the sound pressure level for rock.
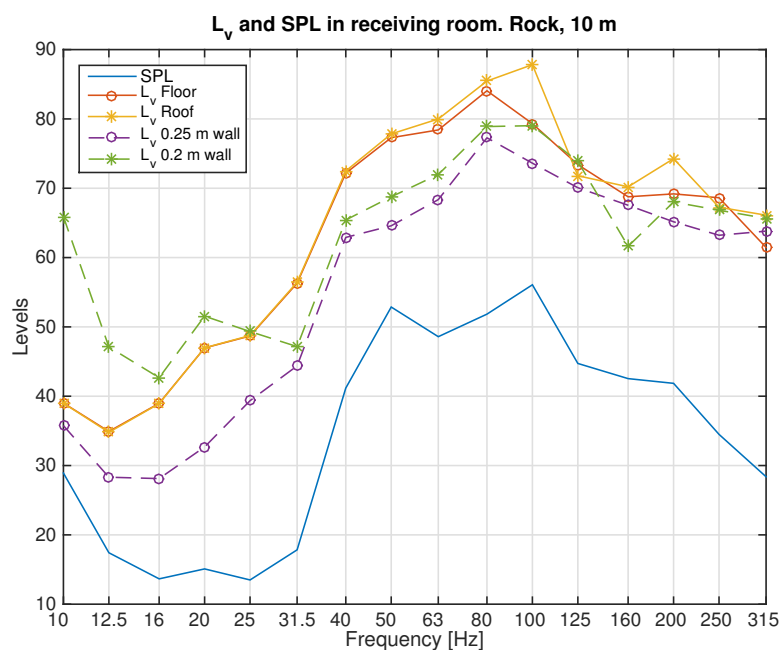

Figure 5.14: SPL in air [dB re. 20 μPa] (not A-weighted) and vibration velocity levels in surfaces [dB re. 1 nm/s] of the receiving room for the case of rock 10 m.
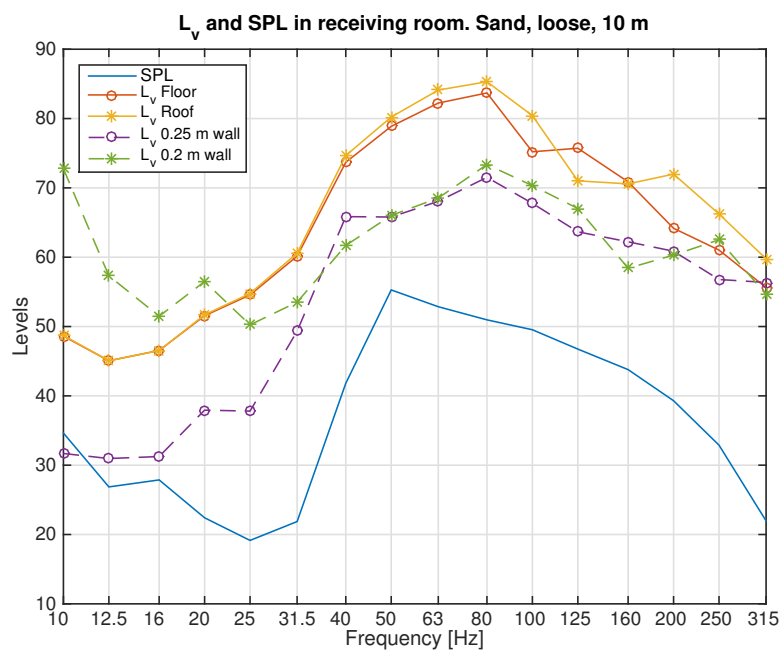
Figure 5.15: SPL in air [dB re. 20 μPa] (not A-weighted) and vibration velocity levels in surfaces [dB re. 1 nm/s] of the receiving room for the case of loose sand 10 m.

6

Discussion

6.1 Low levels

The absolute values of the re-radiated ground-borne noise, presented in figure 5.4, are lower than expected. [Ham 04] lists measured levels for the tunnel Gårdatunneln in Gothenburg. The tunnel goes through rock. At one measurement site with distance 45 m from building to upper edge of the track, $L_{p,ASmax}$ is stated to be 37-38 dBA. The simulation in this study for 40 m rock, gives the value 28.7 dBA. In other words this implies a difference of around 9 dB. It should be noted that the simulated distances, 10-50 m, are the distances between the outer wall of the tunnel and the basement floor. In the model the tunnel is placed vertically straight below the building. The distance to the point of excitation is 7.5 m longer (the height of the tunnel above the rail). When comparing the obtained results from this study to other prediction models or measured values it is important to note which distance is considered.

For the values relative to rock, the fact that the absolute values are low does not matter since the simulations use exactly the same excitation mechanism, tunnel design, building design etc. The only difference is the type of ground between tunnel and building, why the relative values represent the change in levels due to insertion of soil at a location where the ground material is rock. Still, there is a point in evaluating the reasons for the low absolute levels.

There are many factors that influence the ground-borne noise and in this case there may be more than one that are responsible for the low levels. Worn rail or wheel roughness profiles are known to cause high noise levels. Possibly, the roughness profile in the simulations represent a situation with relatively even wheel and rail surfaces. Also, the track is running entirely straight in the model and there are no inclinations, so the forces are evenly distributed in the track construction.

Stiffness changes in the track also cause increased vibration levels. The sleeper distance in the model is 0.6 m and the train speed is 80 km/h, why an excitation at 37 Hz should be seen ($f_{sleeper} = \frac{v_{train}}{d_{sleeper}} = \frac{80}{0.6*3.6} = 37$ Hz). The display of the results in 1/3 octave bands, as well as the A-weighting, make it hard to see the contribution from the sleeper pass-by frequency. Other types of excitation such as wheel flats or rail joints have not been simulated in this model and might have resulted in higher absolute levels.

The vehicle used in the simulations is a freight train car. Locomotives are heavier than the cars, and thus provide a bigger load on the track, which would cause higher vibration levels. Using a locomotive instead for the simulations might hence have caused higher levels of ground-borne noise.

6.2   Comparison to the Ungar-Bender method

The difference between the Findwave and the Ungar-Bender method is very clear at the 10 m distance, as shown in figure 5.7. While the Ungar-Bender method predicts a 5 dB damping, the Findwave model gives an increase. At larger distances the two methods' predictions are more similar, figure 5.8.

It is important to keep in mind that both methods are simplifications of reality and none of them can be said to be entirely correct, unless the models are verified with real measurements. The Ungar-Bender method is based on the assumption that the compression wave is entirely responsible for the vibrations in the building. Findwave is much more complex and accounts for contributions from other wave types.

An explanation to why the Findwave model predicts higher levels in the basement floor than in the tunnel wall at the 10 m distance might be due to the geometry of the model. The Ungar-Bender model estimates the damping from the outer wall of the tunnel to the basement floor, where the distance is the shortest. In the Findwave model, possibly the vibration levels are higher on the sides of the tunnel than right on the top of it. To analyse this, it would be necessary to study and compare the vibration levels above the tunnel along the upper edge of the rock layer, which has not been done in this study.

6.3   Influence of the ground

It seems that the interaction between building and ground matters a lot to the variation of vibration velocity in the different floors of the building. Half of the building is below ground and the other half above. Possibly, the stiffness of the rock allows very little motion of the basement, whereas the upper floor is free to move. In the loose soils, the basement can move more freely relative the ground, why the difference in motion between upper floor and basement is not as big. This could be the explanation to the 100 Hz peak in the ground-borne noise in the case of rock, see figure 5.2, which seems to be due to the peak in the vibration velocity of the roof at the same frequency, figure 5.14. The dense soils, which are stiffer than the loose soils, yet not as stiff as rock, also have a peak in the ground-borne noise level at 100 Hz, but it is not as strong. The peak is entirely gone in the loose soils, as can be seen in figure 5.15.

Equation 3.14 was used to see in any resonances could be expected. The first and second resonances, which are supposed to be the strongest, were calculated for each of the soils. The only resonances that appeared in the frequency region of ground-borne noise were the second resonances of the dense soils, 33.8 Hz for dense clay and 39.4 for dense sand. These resonances cannot be distinguished in the ground-borne noise however.

6.4   Application of the calculated correction factors

The correction factors have been calculated as the difference between the ground-borne noise level from propagation in rock and different soils. The insertion of soil does not just introduce more material damping; it also introduces impedance changes at the edges of the soil, which cause reflections and refractions. This happens at the border between the rock layer and propagation layer and between the building and propagation layer. In other words, the correction factor has accounted for higher level of complexity than just changes in the material damping. The applicability of these results to other situations depends a lot on geometrical aspects as well as material aspects.

The soils in this study are homogenous, meaning the properties remain the same throughout the entire depth. In reality, the soil may consist of different layers, which causes other wave propagation behaviour. Also, in unsorted soils, such as till, it is possible that there may be bigger separates such as cobbles and boulders randomly located in the soil, which also cause other wave behaviour. In other words, the assumption that the soils are entirely homogenous might give other results than reality. It should also be noted that the values for density, compression wave speed and shear wave speed that were used for the soils were listed as properties of water saturated soils, meaning that in cases with soils that are not saturated, different values might be expected. It is clear from this study that the choice of value for the loss factor has a considerable influence on the ground-borne noise, see figure 5.6. The studied soils were all assigned the value 0.05. If the correction factor is used for a soil type that has a higher loss factor, some more damping is expected and the opposite for a soil with a lower loss factor.

The tunnel goes through rock and its cross section is a semi-circular arc. Moreover, the tunnel is just wide enough for one track. Other tunnel designs and constructions principles need to be modelled and simulated to see if the results from this study are applicable also in those cases. The same goes for the building. The building is a one-floor building with basement and slab foundation. It is not known if the results would hold also for a larger building, neither in the case of other foundation types, such as deep foundation. The influence of adjacent buildings is another parameter that has not been studied here.

The peak at 100 Hz that appears in the rock simulations is probably to a resonance in the building, and possibly somewhat amplified by room modes. Figure 5.12 shows that the vibration velocity in the roof has its highest value at 100 Hz. No such peak can be seen in the corresponding figure for the loose sand, figure 5.13. This is also reflected in the figures for the ground-borne noise, for instance figure 5.1, where the loose soils have no peak at 100 Hz. This peak has a big influence on the total level and is accounted for in the correction factors. Hence, there is a risk that the correction factors cause false results if applied to other types of buildings.

7
Conclusion

Correction factors accounting for the insertion of different soil types have been calculated that can be applied to a prediction model for ground-borne noise that is designed to work for rock as propagation material. These factors to be subtracted are found in table 7.1.

Table 7.1: Correction factors to be subtracted from prediction model developed for the case of rock.

Material	$L_{corr,soil}$ [dB] at distance				
	10 m	20 m	30 m	40 m	50 m
Sand, loose	2.1	3.3	3.7	3.7	3.9
Sand, dense	-1.0	0.3	1.5	1.7	2.5
Clay, loose	1.8	2.9	3.2	3.2	3.4
Clay, dense	0.5	2.4	2.7	3.2	4.2

The correction factors have been calculated from a Findwave model that simulates ground-borne noise from a train in a tunnel through rock vertically straight below a one floor building with basement. The software used has been proven to give predictions that are close to measured values, why the software and the theory it is based on should give proper results. In other words, the simulations should give valid results for the case that is modelled. However, without performing measurements at sites similar to the models used in this study, the results cannot be truly validated. The only comparison to measured results in Gårdatunneln indicate that the absolute levels predicted are low, however the only information about that site is distance and that the tunnel is through rock. At the compared distance, the measurement stated a 9 dB higher level than what was predicted in the simulations. A difference in roughness profile for instance could possibly explain the difference in levels. In other words, too little is known about that situation to be able to fully compare it to the prediction.

The model used for the study contains some simplifications that separate it from a real scenario. These include some adaptations of the track sizes to fit the cell size of the model. Also, material simplifications have been done. The soil is assumed to be homogenous throughout the entire depth, which means that the results may not be valid for instance in clays with different layers or till. The influence of the loss factor turns out to be considerable, see figure 5.6, why the results are not expected to be the same for sands of clays with other loss factors. Since the building turned out to have a notable impact on the ground-borne noise spectra, the acquired values for other rooms and especially other buildings might differ.

The method of computer modelling is very convenient, since it can be done in an office and an enormous amount of different scenarios can be simulated. Making a huge number of simulations in order to expand an empirical model is of course time consuming, but compared to making in situ measurements, it requires less effort. The problem is however, that the predicted results need to be validated in some way and the most trustworthy validation is to compare the results to measurements.

Bibliography

[Aas 07] Aasvang, G.M., Engdahl, B., Rothschild, K. (2007) *Annoyance and self-reported sleep disturbances due to structurally radiated noise from railway tunnels*Applied Acoustics, vol. 68, no. 9, pp. 970-981.

[Cre 05] Cremer, L., Heckl, M. & Petersson, B.A.T. (2005) *Structure-borne sound: structural vibrations and sound radiation at audio frequencies* 3rd edition. Berlin; New York: Springer

[Cro 04] Crossrail (2004) *Groundborne Noise and Vibration Prediction; Validation on DLR Greenwich; Technical report* Report no. 1E315-G0E00-00002. London: Cross London Rail Links Limited

[FoH 14] Folkhälsomyndigheten (2014) *FoHMFS 2014:13 Folkhälsomyndighetens allmaänna råd om buller inomhus* Folkhälsomyndigheten, Stockholm.

[Fre 09] Fredén, C (2009) *Sveriges nationalatlas: Berg och jord* 3rd edition. Bromma: Sveriges Nationalatlas.

[Hal 70] Hall, J.R., Richart, F.E., Woods, R.D. (1970) *Vibration of Soils and Foundations* Prentice-Hall. Englewood Cliffs, N.J.

[Hal 12] Hall, L. et alii (2012) *Markvibrationer SGF informationsskrift 1:2012*Swedish Geotechnical Gociety (SGF), SGF's markvibrationskommitté

[Ham 04] Hammarqvist, M. et alii (2004) *Västlänken Underlagsrapport Ljud och vibrationer*Banverket, BRVT 2006:03:10.

[Han 12] Hanson, C. E. et alii (2012) *High-Speed Ground Transportations Noise and Vibration Impact Assessment* Washington, DC: Office of Railroad Policy and Development

[ISO 15] ISO (2014) *Abstract ISO 14837 - 1:2005* http://www.iso.org (2015-08-18)

[Kur 79] Kurzweil, L.G. (1979) *Ground-borne noise and vibration from underground rail systems* Journal of Sound and Vibration, vol. 66, no. 3, pp. 363-370

[Lom 15] Lombaert, G. et alii (2015) Ground-Borne Vibration due to Railway Traffic: A Review of Excitation Mechanisms, Prediction Methods and Mitigation Measures. In *Proceedings of the 11th International Workshop on Railway Noise, Uddevalla, Sweden, 9–13 September 2013* ed. Jens C.O. Nielsen et alii. pp 253-287. Berlin Heidelberg: Springer

[Mel 88] Melke, J. (1988) *Noise and vibration from underground railway lines: proposals for a prediction procedure* Journal of Sound and Vibration, vol. 120, no. 2, pp. 391-406.

[Mul 13] Müller, G. (2013) 9. Structure-Borne Sound, Insulation and Damping. In *Handbook of Engineering Acoustics* ed. M. Möser &. G. Müller, pp 393-487. Berlin Heidelberg: Springer

[SoS 08] Socialstyrelsen (2008) *Buller - Höga ljudnivåer inomhus* Socialstyrelsen, Stockholm.

[Tay 04] Thornely-Taylor, R.M. (2004) *The prediction of vibration, ground-borne and structure-radiated noise from railways using finite difference method- Part1- theory* Proceeding of the Institute of Acoustics. Vol.26. Pt.2 2004. pp 69-79.

[Tem 13] Temple-ERM (2013) *High Speed Rail: Consultation on the route from the West Midlands to Manchester, Leeds and beyond Sustainability Statement Appendix E6 - Noise and Vibration*

[Tho 09] Thompson, D.J., Jones, C., Gautier, P., ScienceDirect (e-book collection) & Knovel (e-book collection) 2009; 2008, *Railway noise and vibration: mechanisms, modelling and means of control*, Elsevier, Amsterdam; Boston.

[Ung 75] Ungar, E.E, Bender, E.K. (1975) *Vibrations produced in buildings by passage of subway trains; Parameter estimation for preliminary design* Inter-noise 75, Sendai, pp 491-498.

[Was 03] Wastensson, G., Öhrström; E., Barregård, L. (2003) *Miljömedicinsk bedömning - Hälsoeffekter av Kust till kustbanans planerade utbyggnad av delen Mölnlycke - Rävlanda/Bollebygd*. Göteborg: Västra Götalandsregionens Miljömedicinska Centrum.

A
Appendix 1

A.1 Material study
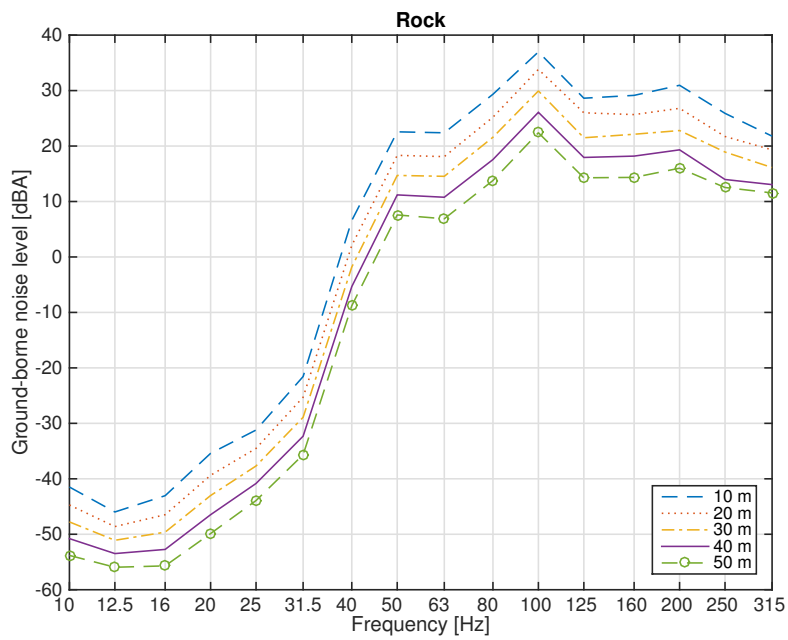
Figure A.1: A-weighted ground-borne noise levels [dB re. 20 μPa], for 10 - 50 m rock.
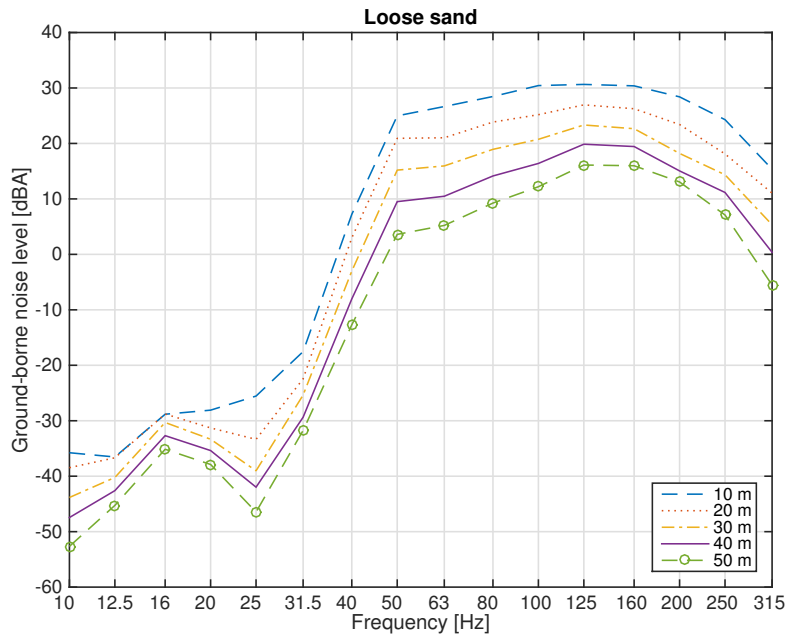
Figure A.2: A-weighted ground-borne noise levels [dB re. 20 μPa], for 10 - 50 m loose sand.
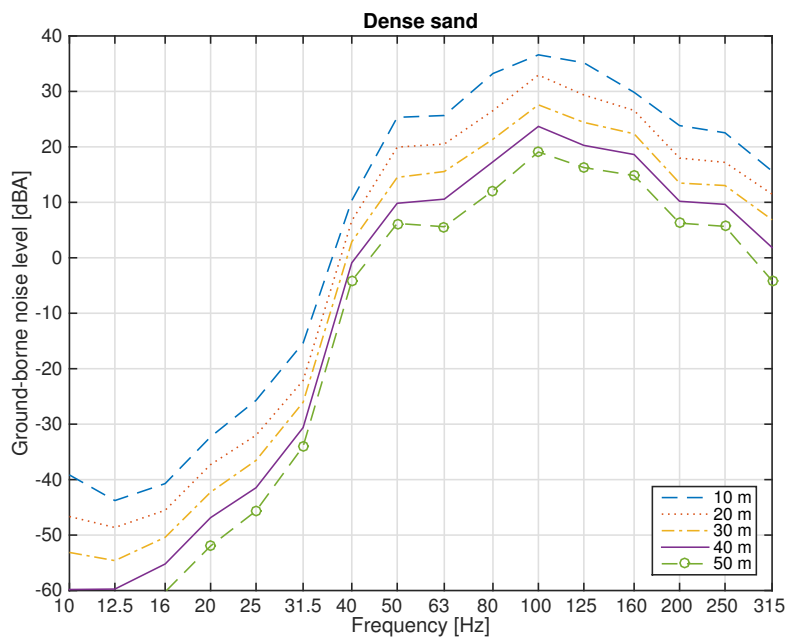

Figure A.3: A-weighted ground-borne noise levels [dB re. 20 μPa], for 10 - 50 m dense sand.
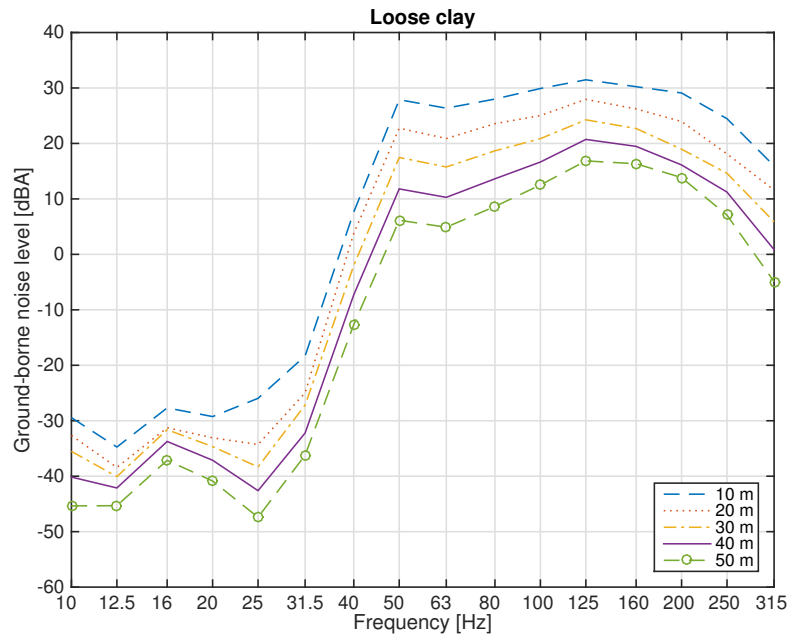
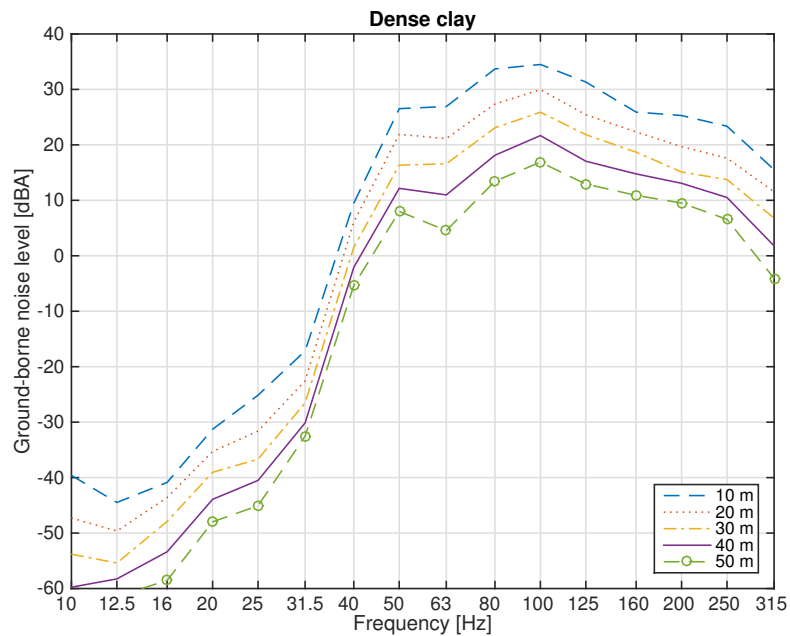**Figure A.4:** A-weighted ground-borne noise levels [dB re. 20 μPa], for 10 - 50 m loose clay.

Figure A.5: A-weighted ground-borne noise levels [dB re. 20 μPa], for 10 - 50 m dense clay.

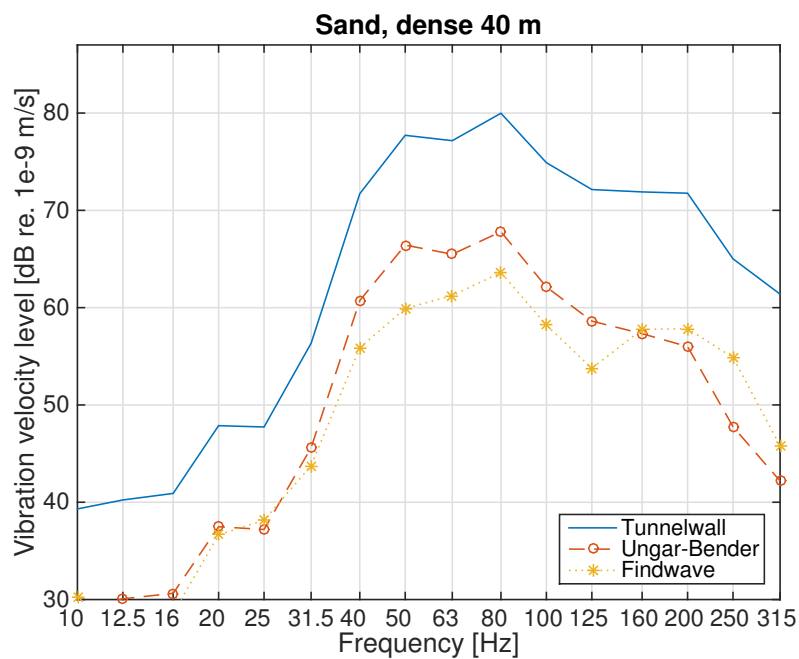## A.2 Ungar-Bender comparison
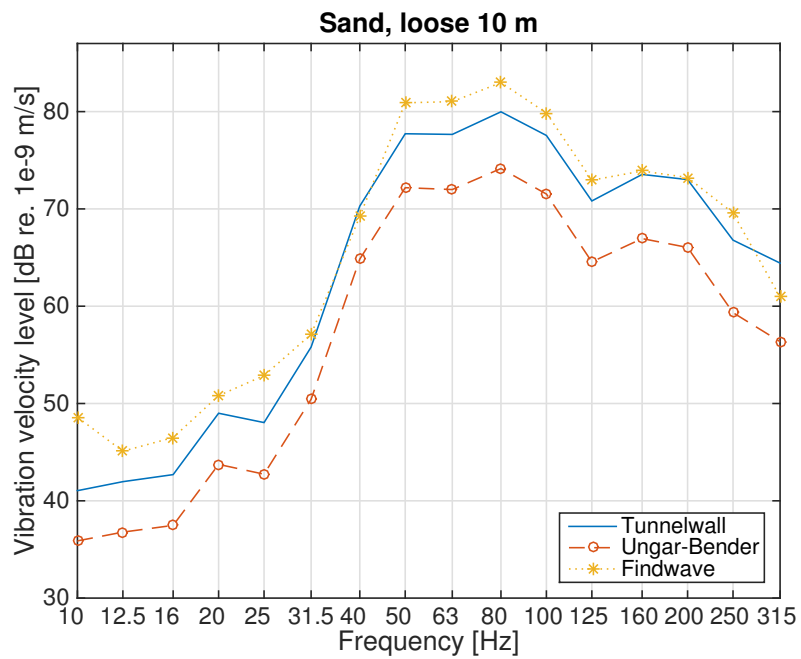
Figure A.6: Comparison of simulated values and calculated values using the Ungar-Bender method for loose sand 40 m. NB! Vibration velocity levels.
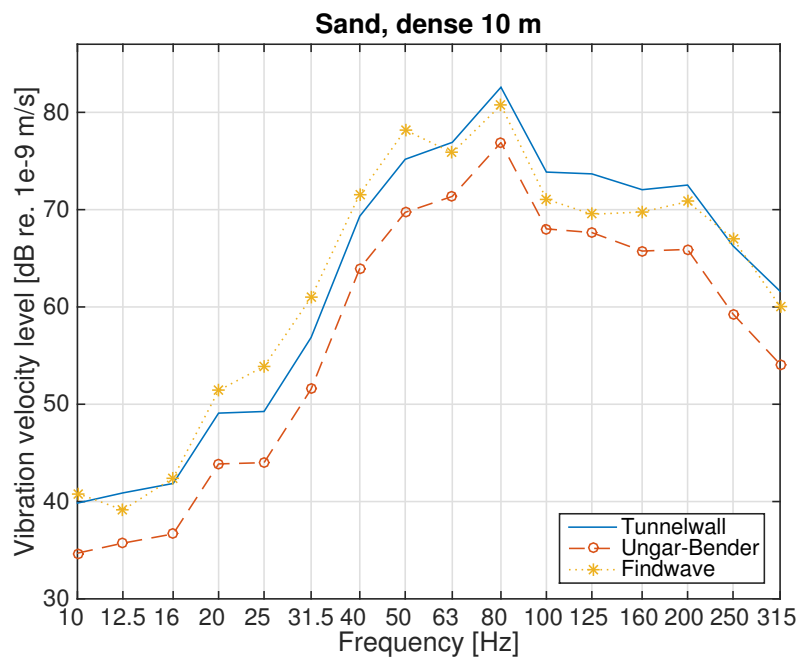
Figure A.7: Comparison of simulated values and calculated values using the Ungar-Bender method for dense sand 10 m. NB! Vibration velocity levels.
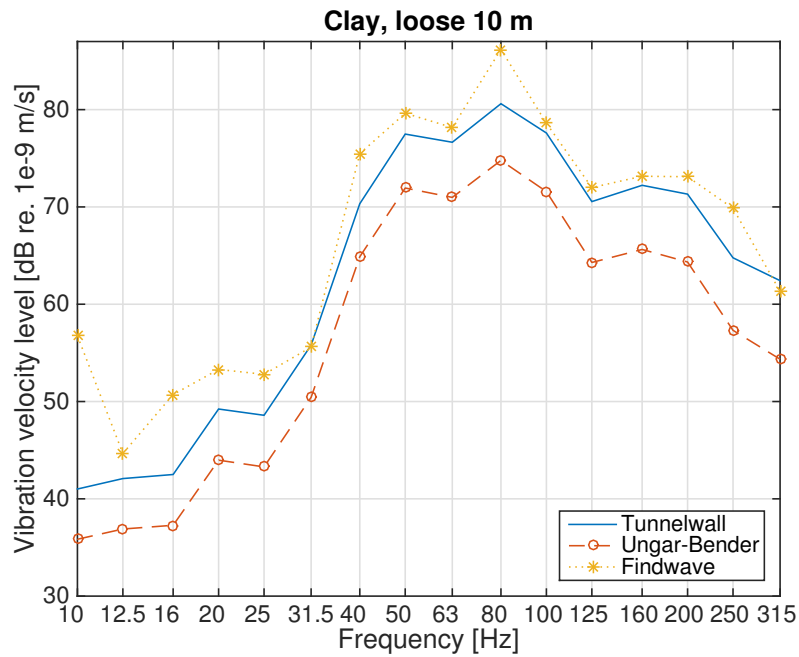

Figure A.8: Comparison of simulated values and calculated values using the Ungar-Bender method for dense sand 40 m. NB! Vibration velocity levels.

Figure A.9: Comparison of simulated values and calculated values using the Ungar-Bender method for loose clay 10 m. NB! Vibration velocity levels.
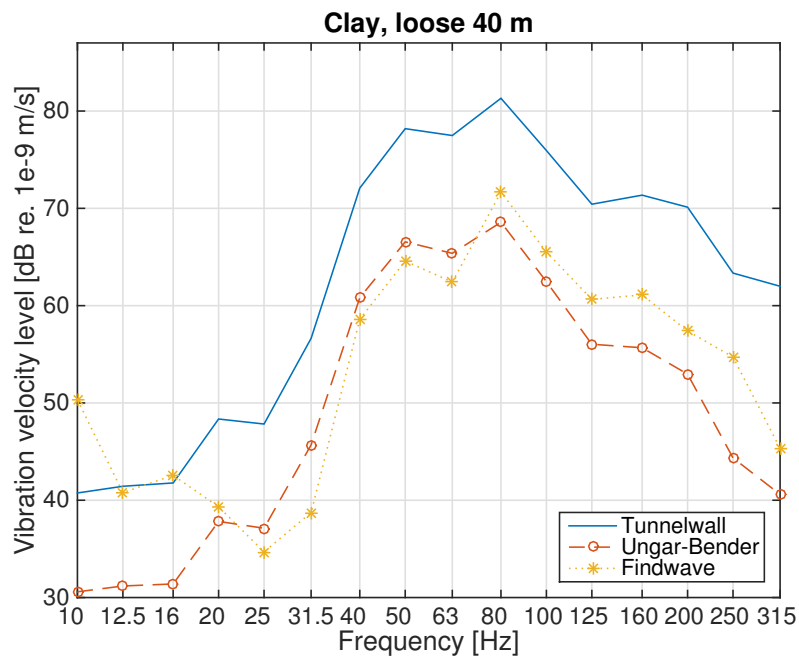

Figure A.10: Comparison of simulated values and calculated values using the Ungar-Bender method for loose clay 40 m. NB! Vibration velocity levels.
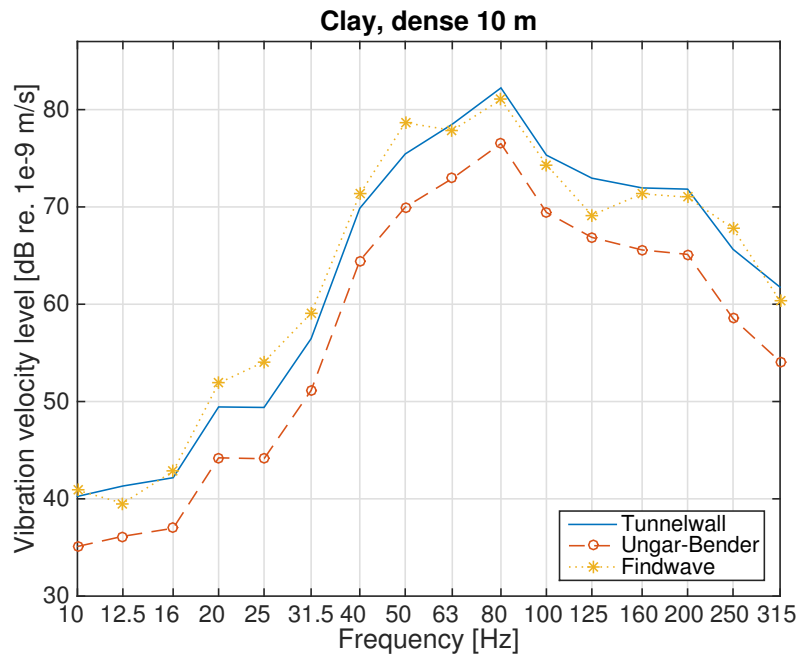
Figure A.11: Comparison of simulated values and calculated values using the Ungar-Bender method for dense clay 10 m. NB! Vibration velocity levels.
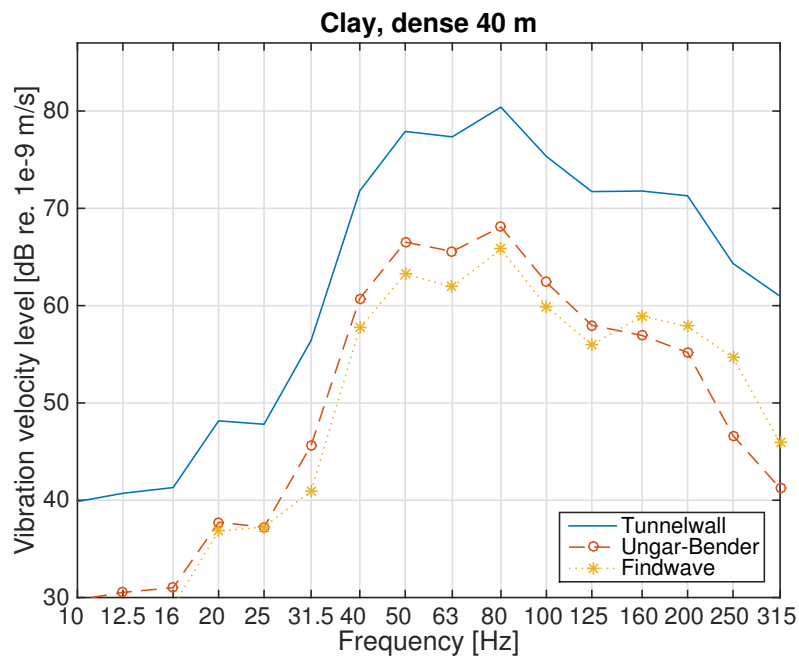

Figure A.12: Comparison of simulated values and calculated values using the Ungar-Bender method for dense clay 40 m. NB! Vibration velocity levels.